Master Thesis

UV and IR properties of Luminous Infrared Galaxies (LIRGs)

University of Crete

Physics Department

section of Astrophysics and Space Physics

Master Thesis manuscript presented by

Alexandros Psychogios

ADVISOR

Vassilis Charmandaris

Heraklio, February 2011

Se ekeinous pou me eixan kai me exoun sthn kardia tous...

Acknowledgments

I am grateful to my supervisor Vassilis Charmandaris for his valuable guidance. I would also like to thank Tanio Diaz Santos for his co-supervision on this project and Thodoris Bitsakis for useful discussions. Finally, I would like to thank my family and my friends for their constant support and encouragement.

Abstract

We used the GALEX data archive of a sample of 12 luminous & ultraluminous infrared galaxies, (U)LIRGs, from the Great Observatories All-Sky Survey (GOALS). UV photometry of these galaxies has been performed to measure the flux densities in the FUV and NUV bands. We also performed the aperture correction photometry of the 3 ULIRGs. Combining our UV measurements with the IR luminosities of Armus et al. (2009) of these galaxies we confirm the following: (U)LIRGs have large infrared excess (IRX) compared to normal starburst galaxies. In general, more luminous (U)LIRGs have larger IRX. The L_{IR} for (U)LIRGs would be underestimated if we tried to measure it using UV measurements and the starburst relation (SR) of Meurer et al. (1999). The deviation above the starburst relation, defined as ΔIRX, increases as L_{IR} increases implying that the decoupling between IR and UV emission becomes greater from LIRGs to ULIRGs. We also examined the star formation rate (SFR) of these galaxies. In particular, the SFR is calculated from the FUV emission and we found that it is only a small fraction, (on average 1.7%), of that obtained from the IR measurements. In order to take into account the extinction that is affecting the UV emission of galaxies we corrected the FUN flux densities for obscuration using two methods: those of Buat (2005) and β(GALEX) slope. Once corrected, the SFR derived accounts for 50.54% and 24.37% of the SFR_{IR}, respectively. We also found that the extinction correction from Buat (2005) is more reliable to (U)LIRGs than the correction with β(GALEX). Finally, the ratio of $\frac{SFR_{IR}}{SFR_{UV\,dustcorrected}}$ increases as the L_{IR} increases for (U)LIRGs. Therefore, the SFR of (U)LIRGs based on UV measurements underestimate their true SFR.

Table of contents

Acronyms

ACS	*Advanced Camera for Surveys*
AGN	*Active Galatic Nucleus*
AAO	*Australian Astronomical Observatory*
BGS	*Bright Galaxy Sample*
BH	*Black Hole*
BLRG	*Broad-Line Radio Galaxy*
BLR	*Broad Line Region*
BL Lac	*Type of AGN*
COBE	*Cosmic Background Explorer*
EM	*ElectroMagnetic*
FIR	*Far Infrared*
FUV	*Far Ultraviolet*
FWHM	*Full Width Half Maximun*
GALEX	*Galaxy Evolution Explorer*
HST	*Hubble Space Telescope*
IC	*Index Catalogue*
IR	*Infrared*
IRAS	*InfraRed Astronomical Satellite*
ISM	*Inter Stellar Medium*
ISO	*Infrared Space Observatory*
LINER	*Low-Ionization Nuclear Emission-line Region*
LIRG	*Luminous Infrared Galaxy*
LMC	*Large Maggelanic Cloud*
MIPS	*Multiband Imaging Photometer for Spitzer*
MIR	*Mid Infrared*
NGC	*New General Catalog*
NLRG	*Narrow-Line Radio Galaxy*
NIR	*Near Infrared*
NUV	*Near Ultraviolet*
OVV	*Optical Violent Variable*
PAH	*Polycyclic Aromatic Hydrocarbon*

PSF	*Point Spread Function*
QSO	*Quasi Stellar Object*
QSR	*Quasi Stellar Radio-source*
SB	*Starburst*
SED	*Spectral Energy Distribution*
SF	*Star Formation*
SFR	*Star Formation Rate*
SMC	*Small Maggelanic Cloud*
SR	*Starburst Relation*
ULIRG	*Ultraluminous Infrared Galaxy*
UV	*UltraViolet*

List of figures

List of tables

Chapter 1

Introduction

In this chapter we present basic information about IR and UV light, galaxies and finally about LIRGs and ULIRGs.

1.1 Infrared light

Infrared light is an invisible part of the electromagnetic spectrum that has wavelengths at the range from 0.7μm to 1mm (longer wavelengths than visible).
In Astronomy, we use the following division scheme :

- Near Infrared, NIR, the region between 0.78 and 3 μm.
- Mid Infrared, MIR, the region between 3 and 50 μm.
- Far Infrared, FIR, the region between 50 and 1000 μm.

The history of IR is associated with a great German musician and astronomer, Sir Frederick William Herschel (1738-1822). Herschel was born in Hanover. When he was 19 years old, he emigrated to England where he constructed telescopes to survey the night sky. His work resulted in several catalogs of double stars and nebulae. William Herschel is perhaps most famous for his discovery of the planet Uranus in 1781.
In the year 1800, he was interested in learning how much heat passes through the different colored filters. Herschel directed sunlight through a glass prism to create a spectrum. A rainbow was created when light divided into its colors. He measured the temperature of each color. He used three thermometers with blackened bulbs (to better absorb the heat) and placed one bulb in each color while the other two were placed beyond the spectrum as control samples. Herschel decided to measure the temperature just beyond the red portion of the spectrum in a region apparently devoid of sunlight. To his surprise, he found that this region had the highest temperature of all.

Herschel performed further experiments on what he called the "calorific rays "that existed beyond the red part of the spectrum and found that they were reflected, refracted, absorbed and transmitted just like visible light. Sir William Herschel had discovered a form of light (or radiation) beyond red light. These "calorific rays "were later renamed infrared rays or infrared radiation, because they are beyond the red part of the spectrum.

Herschel's experiment was important not only because it led to the discovery of infrared, but also because it was the first time that someone showed that there were forms of light that we cannot see with bare eyes.

Generally, it is known that the study of the astronomical objects is based on the information from their light. IR light, as a part of the spectrum, is a useful tool for the study of the celestial objects. In contrast with the optical light, only a small amount of the IR radiation reached the Earth's surface. The reason is that the Earth's atmosphere blocks the IR. In particular, water vapor and carbon dioxide absorb the IR light. Only through a few narrow wavelength ranges the IR light can make it (at least partially) to ground based telescopes. For this reason, space-based IR satellites are better suited to obtain IR observations.

1.2 Ultraviolet light & GALEX satellite

Ultraviolet (UV) light, on the other hand, is the part of electromagnetic spectrum which lies beyond the visible light. The UV wavelengths are in the range of 100Å to 4000Å ($3.5eV$ to $124eV$).

The discovery of UV radiation was made in 1801 from a German physicist, called Johann Wilhelm Ritter. He made the hallmark observation that invisible rays, just beyond the violet wavelength, were especially effective at darkening silver chloride-soaked paper.

In Astronomy, UV emission is interesting because young stars emit most of their light in the UV. In particular, UV radiation comes from the stellar atmospheres of these young stars. There are young stars, called OB associations with masses larger than $10M_{\odot}$. They have temperatures above 10000 K and they are extremely luminous, greater than 25000 $L_{\odot}$. Because they are so massive, OB stars have very hot cores and burn their hydrogen fuel very quickly. According to that, their lifetime is only a few Myr. OB stars are ζ Orionis and Rigel, in the constellation of Orion.

Like the IR light, we cannot observe UV light with ground-based telescopes. The Earth's ozone layer blocks almost all the UV radiation. So, observations at these wavelengths must be performed from space by satellites, such as the GALaxy Evolution

eXplorer (*GALEX*).

GALEX is a program of NASA. *GALEX* provides information about galaxies which have redshift up to z∼2. Its mission is to reveal how galaxies evolve and change. Observing the UV light, mostly produced by the young stars, *GALEX* investigate among others, the causes of star formation (SF) during a period when most of the stars and elements we see today had their origins. It is conducting several sky surveys producing the first comprehensive map of the universe in the UV allowing us to understand how galaxies were formed.

GALEX is a Ritchey-Chretien, 0.5m diameter telescope with 2 detectors in FUV and NUV. Each one has 2 channels, one for imaging and one for spectroscopy. The FUV detector observes the sky at the range of 1350 to 1750 Å, while the NUV detector observes in the band of 1750 to 2800Å. In the next page, a table with the summary of the instrument characteristics is presented.

Table 1.1: *GALEX* instrument table

Telescope Aperture	50 cm	
Optical Design	Modified Ritchey-Chretien with 4 channels: FUV & NUV Imaging, FUV & NUV Spectroscopy.	
Field of View	1.2 degrees diameter, circular	
Focal Length	3 m	
	FUV Channel	NUV Channel
Band	1350-1750 Å	1750-2800 Å
System angular resolution	6.0 arcsec (80%)	8.0 arcsec (80%)
	4.0 arcsec (FWHM)	5.6 arcsec (FWHM)
Photometric Zero Point (1ct/s) m_{AB}	18.8	20.1

(Note): In the first panel we present the general characteristics of the observators and in the second panel the characteristics of each instrument.

The correlation between IR and UV light of galaxies is of great interest. Young massive stars that are born in a galaxy emit UV radiation. The dust that is located in front of the stars absorbs the UV light, heat and re-emits it at IR wavelengths. So, we cannot observe all the UV light from young stars but a fraction of it. If we know a relationship between UV light, absorption from dust and the re-emmited IR light for the galaxies, we can infer a lot of things about their properties and their evolution.

1.3 Galaxies

Galaxies are the big cities of the Universe. Namely, a galaxy is a compact gravitational object which contains stars, supernova remnants, interstellar medium (ISM) and a large amount of dark matter. The most famous classification of galaxies is the one of Edwin Hublle. In his paper "Extra-Galactic Nebulae ", Hubble proposed that galaxies could be divited into 3 primary categories according to their appearence in optical light :

- elliptical galaxies (E)
- spiral galaxies
- irregular galaxies (Irr)

The spirals (S) are further divided into 2 parallel sequences :

- the normal spiral galaxies (S) and
- the barred spiral galaxies (SB)

Between ellipticals and spirals,there is a transitional class of galaxies known as lenticulars. These, can be normal (SØ) or barred (SBØ).
Hubble, explored all the previous groups of galaxies in the form of a tuning-fork diagram shown in figure 1.1.

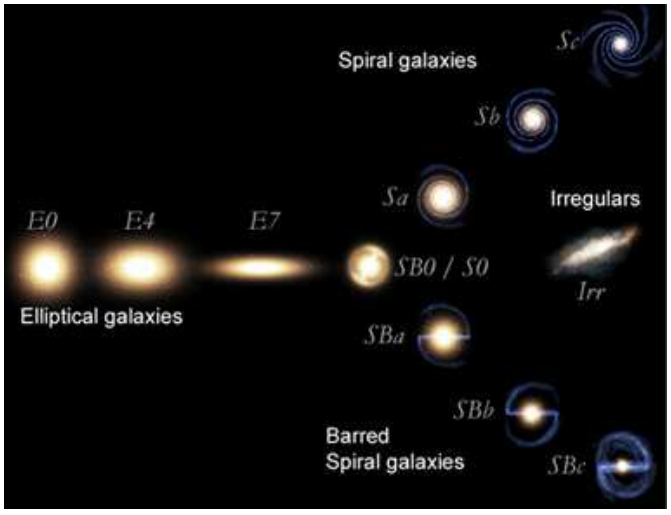

Figure 1.1: Hubble's tuning fork diagram

Hubble, influenced by the tuning-fork diagram, thought incorrectly that the diagram could be interpreted as an evolutionary sequence for galaxies. So, he referred to galaxies toward the left of the diagram as *early* types and those toward the right as *late* types, terminology that is still widely used today.
The elliptical galaxies range from a spherical distribution of stars, named E0, to a highly flattened distribution, named E7. They have old stars (population II) and a small fraction of cool gas. Spiral arms or dust lanes do not exist in elliptical galaxies. Their diameter can be as small as a few tenths of kpc or as large as hundrends of kpc. Their masses vary from as little as 10^7 $M_\odot$ to more than 10^{13} $M_\odot$. The giant ellipticals, which are among the largest objects in the universe, the so called cD galaxies, are found at the center of rich clusters of galaxies while the smallest ellipticals, which are the most numerous of all the galaxies, as dwarf elliptical (dE) and dwarf spheroidals (dSph) are comparable in size to a typical globular cluster.

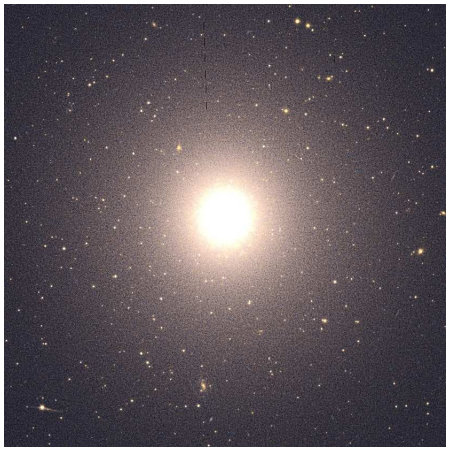

Figure 1.2: The elliptical galaxy NGC1407 as observed with the ACS/WFC Hubble Space Telescope in the B (blue) and I (NIR) filters

The most common type of galaxy (about 55 %) is a spiral galaxy Gisler (1980).
Spiral galaxies are flattened objects with a thin disc. They have long arms winding toward a bright bulge at the center of the disc. There are some spiral galaxies which have a bright bar running through them. These are called barred spiral galaxies (SB). Spiral galaxies are further classified by how tightly their spiral arms are wound. In particular, a spiral galaxy with very tightly wound arms called type SBa. A type SBb galaxy has more loosely wound arms and finally, a type SBc galaxy has very loosely wound arms.

The arms of a spiral galaxy have lots of gas and dust, and they are often areas where new stars (OB association) are forming. The bulge of a spiral galaxy is composed primarily of old stars and very little star formation takes place in the bulge. Their diameter can be as small as a few kpc or as large as tens of kpc. Their masses vary from $10^9 M_\odot$ to more than $10^{11} M_\odot$.

Figure 1.3: The spiral galaxy NGC3370 as observed with the ACS Hubble Space Telescope

Lenticulars are disk galaxies without any conspicuous structure, like spiral arms, in their disks and they lack young stars and gas. This is probably because they have used up most of their gas content in order to consist of old stars only. The lenticular galaxies have masses and luminosities comparable to that of the large ellipticals.

Finally, any galaxy with a strange, peculiar shape and without structure, is an irregular galaxy. Hubble split the irregulars into Irr I if there was at least some hint of organized structure, such as spiral arms, and Irr II for the most disorganized structures.

Irregular galaxies have a lot of gas and dust ($0.5 \leq M_{gas}/M_{total} \leq 0.9$). Furthermore, Irr galaxies sometimes exhibit bars that are off-center. They tend not to be particularly large (their diameters range from 1 to 10 kpc) and they have masses between $10^8 M\odot$ and $10^{10} M\odot$.

1.4 Active Galaxies (AGN)

Apart from the previous types of normal galaxies there are galaxies which present a special characteristic: they have an active nucleus in their central region. From this

Figure 1.4: The lenticular galaxy NGC3115 as observed with the Canada-France-Hawaii Telescope.

Figure 1.5: The left figure shows the Large Maggelanic Cloud (LMC, Irr I) and the right figure the Small Maggelanic Cloud (SMC, Irr II) from the Australian Astronomical Observatory (AAO) by David Malin.

nucleus we observe radiation that is neither starlight emission nor emission from the gas heated by stars. It is important to note that the most powerful AGNs, the quasars, easily outshine their host galaxies.

Active nuclei emit strongly over the whole electromagnetic (EM) spectrum from radio wavelengths to X-rays and γ-rays. In contrast, normal galaxies barely radiate at all the wavelengths.

The emitting region of an AGN may be no bigger than the solar system. Its power source is probably the energy released by gas falling into a central black hole. Very luminous active nuclei, such as quasars, were far more common when the universe was 20% - 40% of its present age. A typical classification of AGN, with their subclasses and characteristics, is the following :

- Seyferts

  Seyfert galaxies which account for $\sim 10\%$ of all galaxies Ho et al. (1997), constitute one of the two main classes of AGNs (the other class being the more radio-loud quasars). Although sometimes associated with enhanced star-burst activity, a Seyfert nucleus, by definition, contains an AGN and exhibits this via the presence of a non-stellar nuclear source. Often, unlike star-burst galaxies, the Seyfert nuclei are associated with radio or optical jets. These galaxies are divided into two main classes according to their optical properties: type 1 and type 2 Seyferts. The main difference between these classes is that, in addition to the narrow line emission evident in both the main classes, type 1 Seyferts also exhibit broad line emission, which covers a wide range of ionisation, as Wilson et al. (1993) state. The narrow lines (widths $\sim 10^2$ km s^{-1}) are believed to be due to low density ($n_e \sim 10^3$-10^6 cm^{-3}) gas clouds relatively far from the core which are ionised either by photoionisation from the central source or by shock excitation from the radio jets emanating from the core Dopita & Sutherland (1995). The broad lines (widths $\lesssim 10^4$ km s^{-1}) result from dense ($n_e \lesssim 10^9$ cm^{-3}) photoionised gas clouds, orbiting close to the central power source (Robson 1996).

- Quasars

  Quasars are compact-looking objects, often radio sources, with emission lines in their spectrum which are displaced by very large amounts towards the red. These redshifts correspond to velocities which are a large fraction of the speed of light, and hence these objects are believed to lie at great distances (McLean 1997) Quasars may be the central regions of very energetic galaxies at an early stage of their evolution. It is believed that the power of a quasar derives from a massive black hole at its center. Quasars split in two categories with respect to their radio emission. Quasi stellar radio-source (QSR) are variable sources with broad and narrow emission lines, strong radio emission with some polarization. In contrast, quasi stellar object (QSO) present broad and narrow emission lines but wike radio emission with weak polarization.

- Radio Galaxies

  Radio galaxies are types of active galaxies that are very luminous at radio wavelengths from 10^{34} up to 10^{38} W (L.S.Sparke & J.S.Gallagher). The radio emission is due to the synchrotron process. They have a distinctive structure, with twin radio-bright lobes on either side of the galaxy. The active nucleus is seen as a core radio source, only a few pc across (L.S.Sparke & J.S.Gallagher). Many cores

vary in luminosity over periods of a year or less; so they must be less than a light year across. Narrow bright jets of emission are often seen to emerge from the central core. Some of these are two-sided, while others are visible on only one side of the galaxy. These galaxies turn out to be giant ellipticals and cD galaxies. Radio galaxies are divided in two categories with respect to their emission-line width: Broad Line Radio Galaxies (BLRG) present broad and narrow emission lines with variable radio luminosity. On the other hand, Narrow Line Radio Galaxies (NLRG) present only narrow emission lines and strong radio emission with no variability.

- Blazars

The properties of rapid variability and a high degree of linear polarization at visible wavelengths define the class of AGNs known as *Blazars*. In particular, blazar is a highly variable active galaxy which, in general, displays no emission lines in its spectrum (Clark 1997). The term *blazar* is collectively used to refer to BL Lac objects and Optically Violent Variables (OVVs). The optical spectra of BL Lacs objects are characterized by their rapid time variability. Their luminosities may change by up to 30 % in just 24 hours and by a factor of 100 over a longer time period. BL Lac are devoid of emission lines. However, observations of a few faint spectral lines have revealed high redshifts. About 90% of them appear to reside in elliptical galaxies. The other class of blazars, OVV objects are similar to BL Lacs except that they are typically much more luminous and their spectra may display broad emission lines (B.W.Caroll & D.A.Ostlie).

- LINERs

Low-Ionization Nuclear Emission-line Region (LINER) are galaxies with very low luminosities in their nuclei, but with fairly strong emission lines of low-ionization species, such as the forbidden lines of [O I] and [N II]. The spectra of these galaxies seem similar to the low-luminosity end of the Seyfert 2 class and LINER signature are detected in many spiral galaxies. These low-ionisation lines are also produced in extreme starburst galaxies and in H II regions, so it is unclear whether LINERs truly represent the low-luminosity limit of the AGN phenomena (B.W.Caroll & D.A.Ostlie).

1.5 ULIRGs and LIRGs

A luminous infrared galaxy (LIRG), is a galactic body whose defining characteristic is that it emits more than 10^{11} $L_{\odot}$ in the far-infrared (FIR) part of the electromagnetic spectrum. Accordingly, a more luminous system, emitting more than 10^{12} $L_{\odot}$ in the FIR, is called ultraluminous infrared galaxy (ULIRG) Sanders & Mirabel (1996).

One of the most important issues related to these galaxies is that they may be related to the formation of QSO (Sanders et al. (1988a); 1988b) and powerful Radio-galaxies Mazzarella et al. (1993). They may also represent a primary stage in the formation of elliptical galaxy cores, the formation of globular clusters and the metal enrichment of the intergalactic medium Sanders & Mirabel (1996).
History about these galaxies was start by ground-based observations, during the 70's, which allowed astronomers to show that these objects, which were bright at optical wavelengths, were even brighter at IR. Most of the IR luminosity of these objects proceeds from the UV radiation of young stars. In particular, this UV radiation is absorbed by dust located near the stars and is re-emitted at IR wavelengths with a spectral energy distribution (SED) similar to that of a black body at the same temperature as the emitting dust.

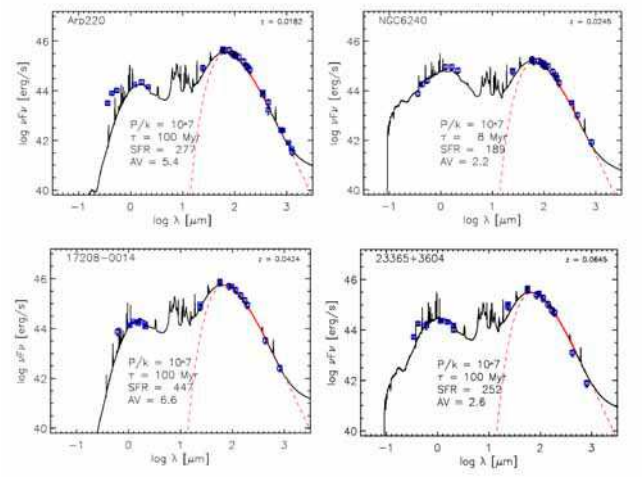

Figure 1.6: The fits to the SEDs of a few well-known ULIRGS in the local universe, scaled to a star formation rate of 1 M$\odot$ year^{-1}, Reuland (2005)

But the revolution came with the observations of the IR satellite called *IRAS* in 1983. This satellite surveyed the sky at IR wavelengths and showed that much of the present star formation is optically obscured). Furthermore, it revealed the population

of LIRGs and ULIRGs and provided the first hints of strong evolution in the number density of ULIRGs at recent cosmic epochs. Also, showed that a large fraction of these IR galaxies are interacting or merger systems. Another considerable step forward was done with the *COBE* satellite in 1989. *COBE* investigated the cosmic FIR background and showed that the energy coming from stars is as important as that coming from dust. That implies that the IR radiation is related to the star formation in galaxies. In 2003, another IR satellite, *Spitzer* observed the sky from 3.6 to 160 μm. The rest of the far IR spectrum (FIR) will be studied with the *Herschel Space Telescope* which was launched in May 2009. *Herschel Space Telescope* will obtain information allowing us to measure the total IR luminosity of these galaxies more accurately.

The morphology of (U)LIRGs ranges from isolated spirals to mergers in an advanced stage of interaction. In particular, at $L_{IR} < 10^{11}$ $L_{\odot}$ the vast majority of IR galaxies appear to be single, gas rich spirals whose L_{IR} can be accounted mostly by star formation.

At the range $10^{11} L_{\odot} \leq L_{IR} \leq 10^{12} L_{\odot}$ there is a dramatic increase in the frequency of strongly interacting systems that are extremely rich in molecular gas and the luminosity appears to be dominated by starbusrts.

Furthermore, galaxies with $L_{IR} > 10^{12}$ $L_{\odot}$ contain exceptionally large concentrations of molecular gas Sanders & Mirabel (1996). Because of heavy dust obscuration, it is hard to distinguish the power source of these objects. Either way, the conditions are optimal for fueling enormous nuclear starbursts as well as building and/or fueling an AGN.

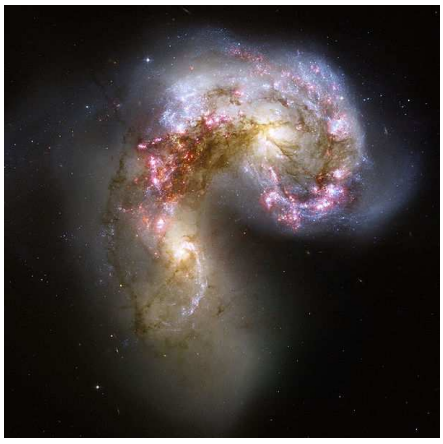

Figure 1.7: The classic, nearby early merger system Arp 244, "the Antennae". The total IR luminosity from this system is the minimun required by our definition of LIRG.

Generally, most LIRGs are late type galaxies which emit a large fraction of their luminosity in IR wavelengths. In particular, their luminosity in the FIR range of spectrum is $10^{11}L_{\odot} \leq L_{IR}[8\text{-}1000\mu m] \leq 10^{12}L_{\odot}$ for LIRGs. ULIRGs emit the 90% of their luminosity in FIR with values of $L_{FIR} \geq 10^{12}L_{\odot}$.

The reason that these galaxies emit a large fraction of their energy in the IR wavelengths is that they contain huge amounts of dust. Dust consists of small grains.
A substantial fraction of the grains are particles which contain up to 100 atoms of carbon and behave like large molecules. These are called Polycyclic Aromatic Hydrocarbons (PAHs; Draine (2003) and are formed on the surface of the grains.
Dust grains (silicate and graphite) absorb the starlight photons. A part of the absorbed light goes into luminescence or ejection of a photoelectron but the major part goes into heating the interstellar grain material. In particular, the NIR/MIR emission must be produced by grains of size 5-50 Å. Such grains are large enough to have an almost continuous density of energy states. In this case they radiate a continuum rather than emission bands. A single UV photon heats the grain to a high peak temperature that depends upon the size of the grain and the energy of the photon. The grain emits the NIR/MIR radiation and cools to very low temperatures between photon absorptions. Grains with sizes of 0.01 μm or more are cold ($\sim$ 20 K) and reradiate most of the energy they absorb into the FIR part of the spectrum.

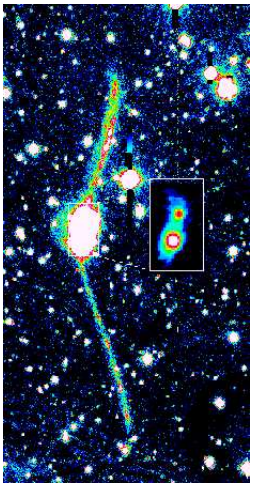

Figure 1.8: "The Superantennae"(IRAS 19254-7245) is a prototype ULIRG. Optical r-band image and inset in the K-band (2.2 μm) of the nuclear regions Mirabel et al. (1991).

Another characteristic of (U)LIRGs is that they are extremely rich in molecular gas (Sanders & Mirabel (1996)). Their total H_2 mass is in the range $\sim$1-30$\times10^9$ $M_\odot$, or approximately 0.7 to 20 times the molecular gas of the Milky Way. The mean molecular gas temperatures and densities in the central regions of (U)LIRGs are hot (T_{kin}=60-90 K) and dense (n(H_2) $\sim$ 10^5-10^7cm^{-3}), similar to the conditions in massive Galactic giant molecular cloud cores, surveyed by Sanders & Mirabel (1996). So, their SFR is very high in comparison with that of normal galaxies. On average, ULIRGs present star formation rates $\sim$ 100$M_\odot$ yr^{-1}. In comparison, our own Galaxy (Milky Way) has the value of $\sim$2-3 $M_\odot$ yr^{-1}.

The power source of the (U)LIRGs, as we report above, is a mixture of AGN and/or a circumnuclear starburst, both of which are fueled by an enormous concentration of molecular gas that has been funneled into the merger nucleus Genzel et al. (1998). In the process of a violent interaction of two spiral galaxies, hydrogen clouds that were initially distributed throughout the galactic disc, could move to the center forcing the gas to become concentrated. Numerical simulations of colliding galaxies Barnes (1992), showed that the gas and stars react differently to the impact of an intruding galaxy. The gas tends to move out in front of the stars as they orbit the galactic center. Furthermore, stars' gravity pulls back the gas, and the resulting torque on the gas reduces its angular momentum, causing it to plunge toward the galactic center. As the two galaxies begin to merge, more angular momentum is lost and the concentrated gas will make new stars, thus fueling a starburst, or make an accretion disk producing an active AGN. This system will pass through a violent stage, when the spiral arms and the disc from both galaxies will be destroyed and the population of the stars will relax to a ($r^{1/4}$) distribution Tacconi et al. (2002) which is the characteristic distribution of an elliptical galaxy.

While (U)LIRGs are rare in local universe, at high redshifts their number density increases. Furthermore, these galaxies play a significant role in star formation (SF) at high redshifts. Several teams during the season 1999-2004, confirmed the importance of IR galaxies for the understanding of SFR evolution (Elbaz et al. (1999); Aussel et al. (1999); Chary & Elbaz (2001); Franceschini et al. (2001); Elbaz et al. (2002); Metcalfe et al. (2003); Lagache et al. (2004)). They all found that the contribution of LIRGs to the SFR density increases with redshift up to z$\sim$1 and that at high redshift the bulk of the SFR density occurs in (U)LIRGs. Le Floc'h et al. (2005), using deep 24μm Multiband Imaging Photometer MIPS (Rieke et al. (2004)) observations with *Spitzer*, obtained a complete census of the SFR density evolution up to z$\sim$1 and found a strong evolution with cosmic time of the relative contributions of normal, LIRG and ULIRG galaxies to the SFR density.

At z∼0 the SFR density is dominated by quiescent galaxies whereas at z∼1 it is dominated by LIRGs. They also found that the contribution of ULIRGs to the SFR density rises steeply from z=0 to z=1 but still remains negligible at z∼1 (i.e. less than 10%). More recently, studies using MIPS 24 μm data have extended previous works to higher redshift and showed that ULIRGs may dominate the SFR density at z∼2 (Caputi et al. (2007)). While the (U)LIRGs dominate the star formation in higher redshifts and to-

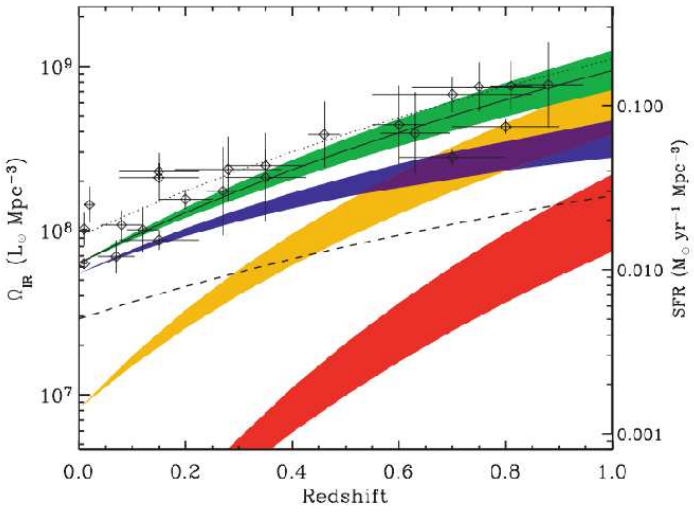

Figure 1.9: Evolution of the comoving IR energy density up to z=1 (green filled region) and the respective contributions from low-luminosity galaxies (blue filled area), IR-luminous sources (orange filled region) and ULIRGs (red filled region). The solid line evolves as $(1+z)^{3.9}$ and represents the best fit of the total IR luminosity density at $0 \lesssim z \lesssim 1$. The dashed line corresponds to the SFR measured from the UV luminosity not corrected from dustextinction. The dotted line represents the best estimate of the total SFR density as the sum of this uncorrected UV contribution and the best fit of the IR-SFR (solid line). At z∼1 IR-luminous galaxies represent 70%±15%of the comoving IR energy density and dominate the star formation activity

gether span all the stages of galaxies, from isolated galaxies to interacting pairs and mergers, it is obvious that these IR galaxies plays a key role in the understanding of the general evolution of the galaxies.

Finally, ULIRGs represent the initial, dust-enshoured stages of quasars. The sufficient evidence of this scenario is the dominant non-thermal ionization as probed by the optical emission lines, the extreme NIR colors and the large $\frac{L_{IR}}{M(H2)}$ ratios which are similar to those of quasars.

Once these nuclei shed their obscuring dust, allowing the AGN to visually dominate the decaying starburst, they become optically selected quasars. The formation of quasars through the merger of molecular gas-rich spirals can account for both the increased number of high-luminosity quasars at large redshift, when the universe was younger and gas supplies less depleted, and the observed "redshift-cutoff "of quasars, which represents the epoch after galaxy formation when the first collisions occured.

Chapter 2

Data & Analysis

In this chapter we present the data of the 12 (U)LIRGs as well as their analysis. Specifically, in the first section we present the data of the 12 (U)LIRGs, in the second section we present the UV photometry of the 12 galaxies and in the 3nd one the procedure of aperture correction for 3 ULIRGs.

2.1 Data

Our sample consists of 12 galaxies, 9 of them are LIRGs and the rest are ULIRGs. All of them were selected from the sample of Great Observatories All-sky LIRG Survey (GOALS; Armus et al. 2009). The GOALS sample is a part of a complete sample of 629 galaxies named Revised Bright Galaxy Sample (RBGS; Sanders et al. 2003). In the table 2.1 I present the general characteristics of the 12 galaxies.

The sample of 12 (U)LIRGs have the form of UV and IR data. In particular, the UV data which I used comes from the GALEX data archive. These files are hosted by the Multi-Mission archive at the Space Telescope Science Institute (MAST). The 12 galaxies were observed as part of the following programs:
NGS (Nearby Galaxies Survey)
DIS (Deep Imaging Survey)
MIS (Medium Imaging Survey)
AIS (All Sky Survey)
GII (Guest Investigator Data)

All galaxies have been observed in both FUV and NUV bands which have effective wavelengths (λ_{eff}) of 1528Å and 2271Å respectively. We use the Intensity Maps (J2000) of FUV and NUV bands which have units of photons/pixel/second, corrected

Table 2.1: General characteristics of the (U)LIRGs

Galaxy	R.A.(J2000) [1]	Dec (J2000) [2]	Distance (Mpc) [3]	$\log(L_{IR})$ [4]
IC 1623	01h 07m 47.18s	$-17°30'25.3''$	85.5	11.71
NGC 877	02h 17m 59.64s	$+14°32'38.6''$	54.6	11.10
NGC 1365	03h 33m 36.37s	$-36°08'25.4''$	17.9	11.00
NGC 23	00h 09m 53.41s	$+25°55'25.6''$	65.2	11.12
NGC 3110	10h 04m 02.11s	$-06°28'29.2''$	79.5	11.37
NGC 1068	02h 42m 40.71s	$-00°00'47.8''$	15.9	11.40
NGC 2342	07h 09m 18.08s	$+20°38'09.5''$	78.0	11.31
NGC 695	01h 51m 14.24s	$+22°34'56.5''$	139.0	11.68
NGC 958	02h 30m 42.58s	$-02°56'27.2''$	80.6	11.20
IRAS F23365+3604	23h 39m 01.27 s	$+36°21'08.7''$	287.0	12.20
IRAS F22491-1808	22h 51m 49.26 s	$-17°52'23.5''$	351.0	12.20
IRAS F15250+3608	15h 26m 59.40 s	$+35°58'37.5''$	254.0	12.08

[1] The best available source right ascension (J2000) in NED as of 2008 October
[2] The best available source declination (J2000) in NED as of 2008 October
[3] The luminosity distance reported in the RBGS in Armus et al. (2009)
[4] The total IR luminosity in $\log_{10}$ Solar units computed using the IRAS flux densities reported in the RBGS in Armus et al. (2009)

for the relative instrument response.

The integration times depend on the surveys. In particular, the files of AIS have integration times of 100s.The integration times of the other surveys (NGS, DIS, MIS, GII) is up to 1500s and so are deeper.

Finally, the 12 galaxies have redshifts ranging from 0.0055 to 0.0777 with a mean of 0.03 which means that are local galaxies. We adopt the following cosmology Ω_Λ=0.72, Ω_m=0.28, with H_0=70 km s^{-1} Mpc^{-1}.

2.2 Photometry

The aim of the UV photometry is to measure the flux densities of the 12 galaxies on the two bands of GALEX: FUV and NUV. To measure the flux densities we used a speciallized routine of IDL, called *atv*. In particular, in order to find the total flux density of each galaxy, the following procedure was adopted:

We measure the flux density inside an aperture and repeat the process for a set of increasing aperture sizes until including the entire galaxy. The set of the apertures, in units of arcseconds, is the following: 1.5, 3.0, 4.5, 7.5, 12.0, 15.0, 19.5, 22.5, 27.0, 30.0 and 37.5. If the size of the source is greater than 37.5 arcseconds, we take extra values of apertures increasing every time by 7.5 arcseconds. To calculate the real flux of the

galaxy we substract the background flux density from the measured flux.

If an image belongs to the surveys NGS, DIS, MIS or GII (high integration time), we can obtain the flux density of a source by automatically substracting the background emission from a ring located beyond the aperture. But in some cases, the background values of the images are very low, especially for the FUV images. In that case we measure the background flux manually following the method:

An annulus outside the source is used, with inner and outer radius relative every time to the size of the galaxy. The flux density inside the annulus is measured and finally, we divide the difference by the area of the annulus. Furthermore, for each galaxy we plot its curve of growth that is the flux density enclosed in each of the apertures defined above, as a function of the aperture size. In the next images, the curves of growth of the 12 (U)LIRGs of FUV and NUV bands are illustrated.

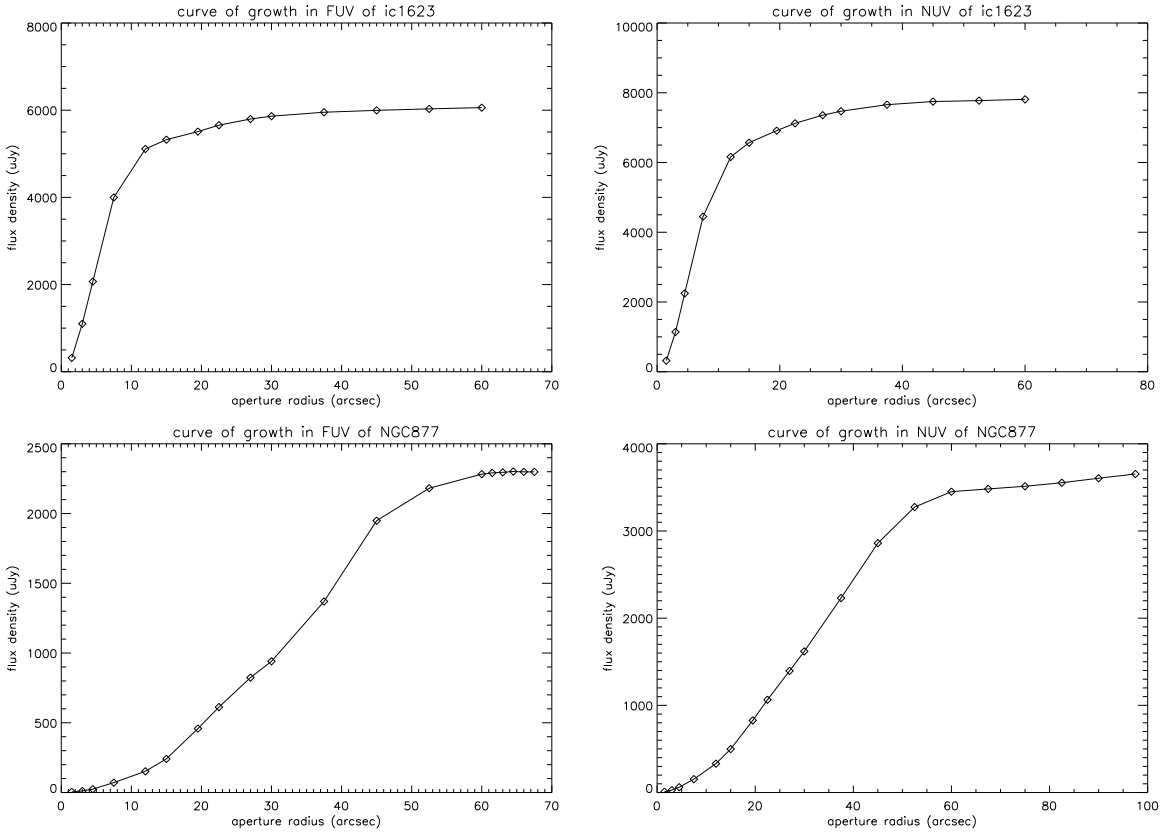

Figure 2.1: Curves of growth from left to right and top to bottom of IC1623 in FUV, IC1623 in NUV, NGC877 in FUV and NGC877 in NUV. The flux density is in μJy and the apertures in arcsec.

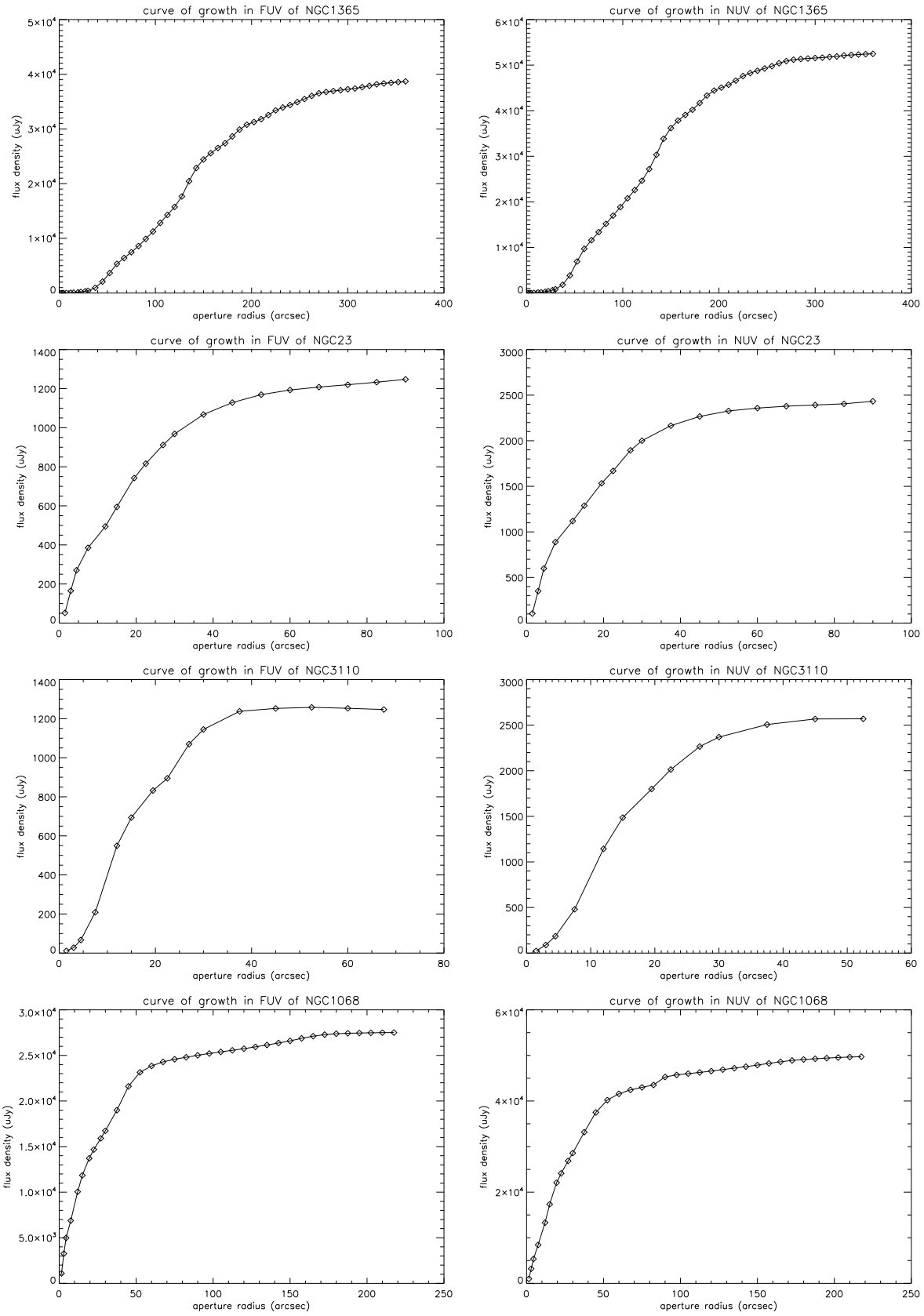

Figure 2.2: Curves of growth from left to right and top to bottom of NGC1365 in FUV, NGC1365 in NUV, NGC23 in FUV, NGC23 in NUV, NGC3110 in FUV, NGC3110 in NUV, NGC1068 in FUV and NGC1068 in NUV. The flux density is in μJy and the apertures in arcsec.

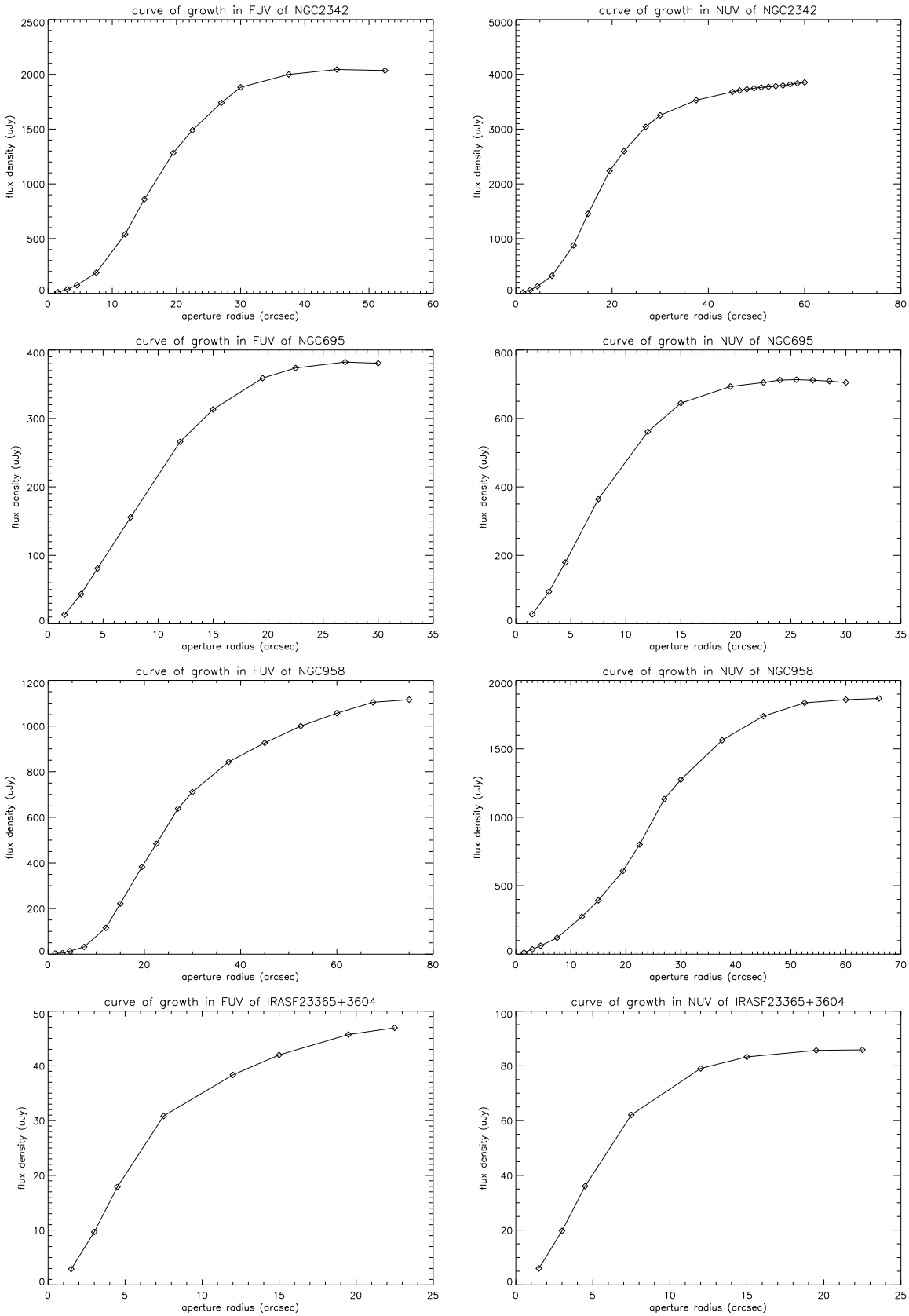

Figure 2.3: Curves of growth from left to right and top to bottom of NGC2342 in FUV, NGC2342 in NUV, NGC695 in FUV, NGC695 in NUV, NGC958 in FUV, NGC958 in NUV, IRASF23365+3604 in FUV and IRASF23365+3604 in NUV. The flux density is in μJy and the apertures in arcsec.

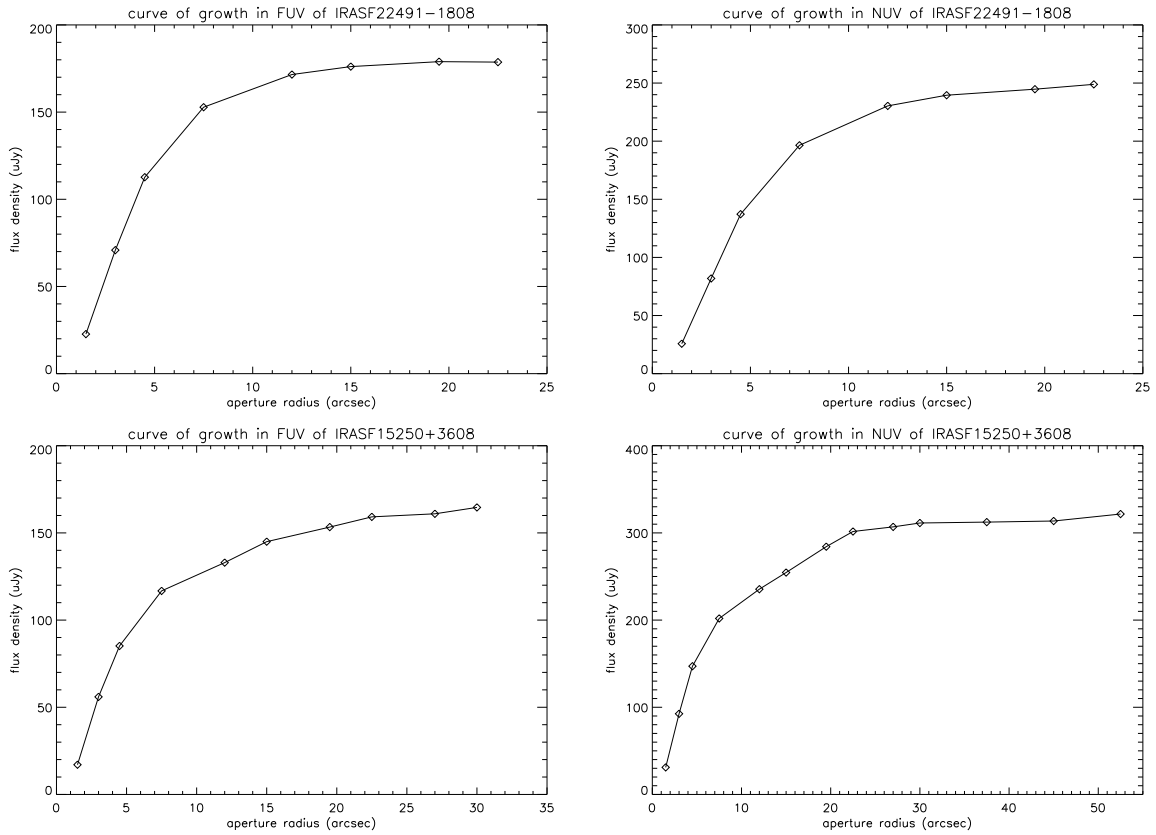

Figure 2.4: Curves of growth from left to right and top to bottom of IRASF22491-1808 in FUV, IRASF22491-1808 in NUV, IRASF15250+3608 in FUV and IRASF15250+3608 in NUV. The flux density is in μJy and the apertures in arcsec.

In the figures 2.5, 2.6, 2.7 and 2.8 the images of the galaxies with the apertures are presented. The three colored apertures (red, blue, green) in the images correspond to the outer and inner sky and to the last aperture for the measured flux density. When the total flux is measured up to the inner sky, the yellow aperture is not shown.

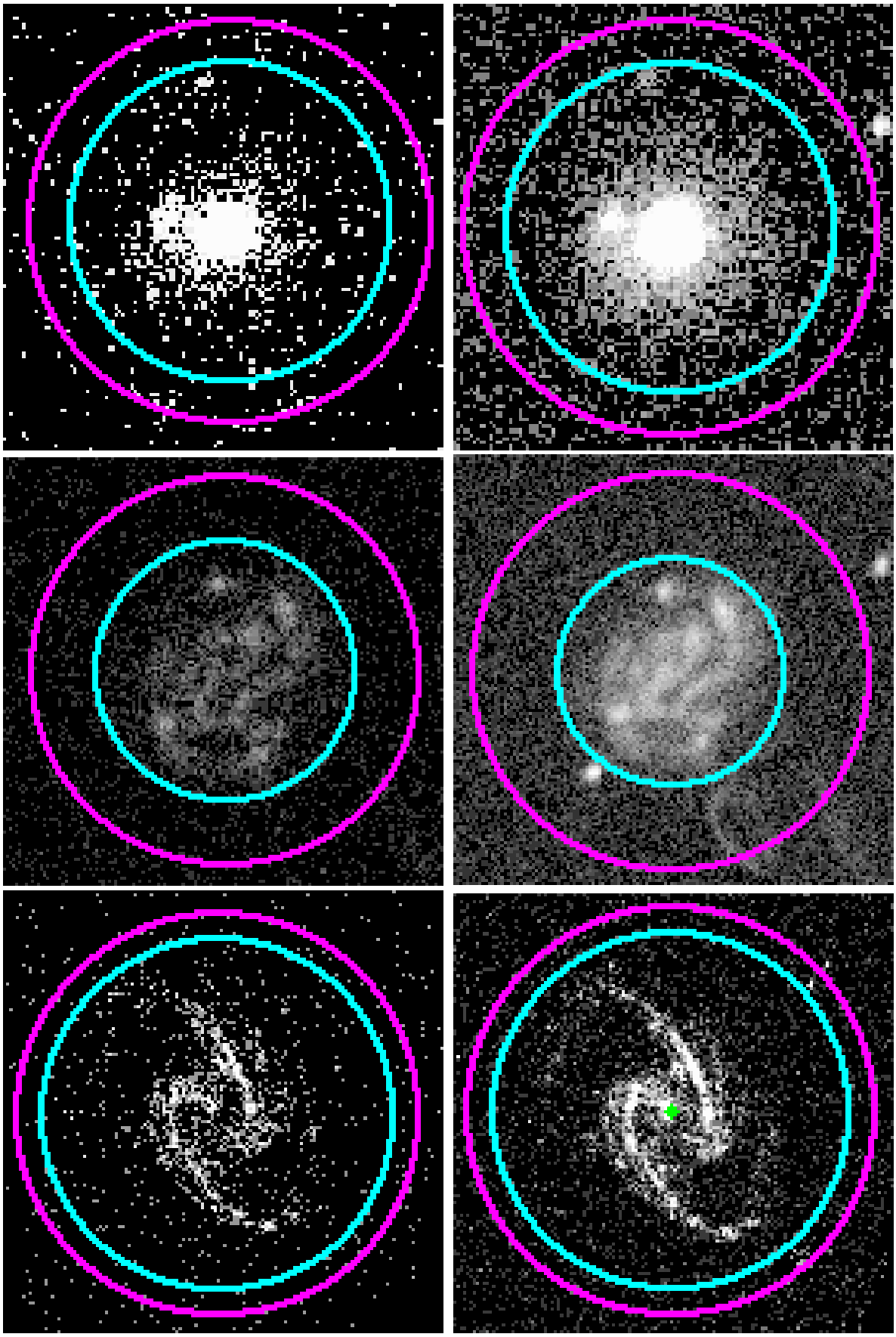

Figure 2.5: Fits images from left to right and top to bottom of IC1623 in FUV, IC1623 in NUV, NGC877 in FUV, NGC877 in NUV, NGC1365 in FUV and NGC1365 in NUV.

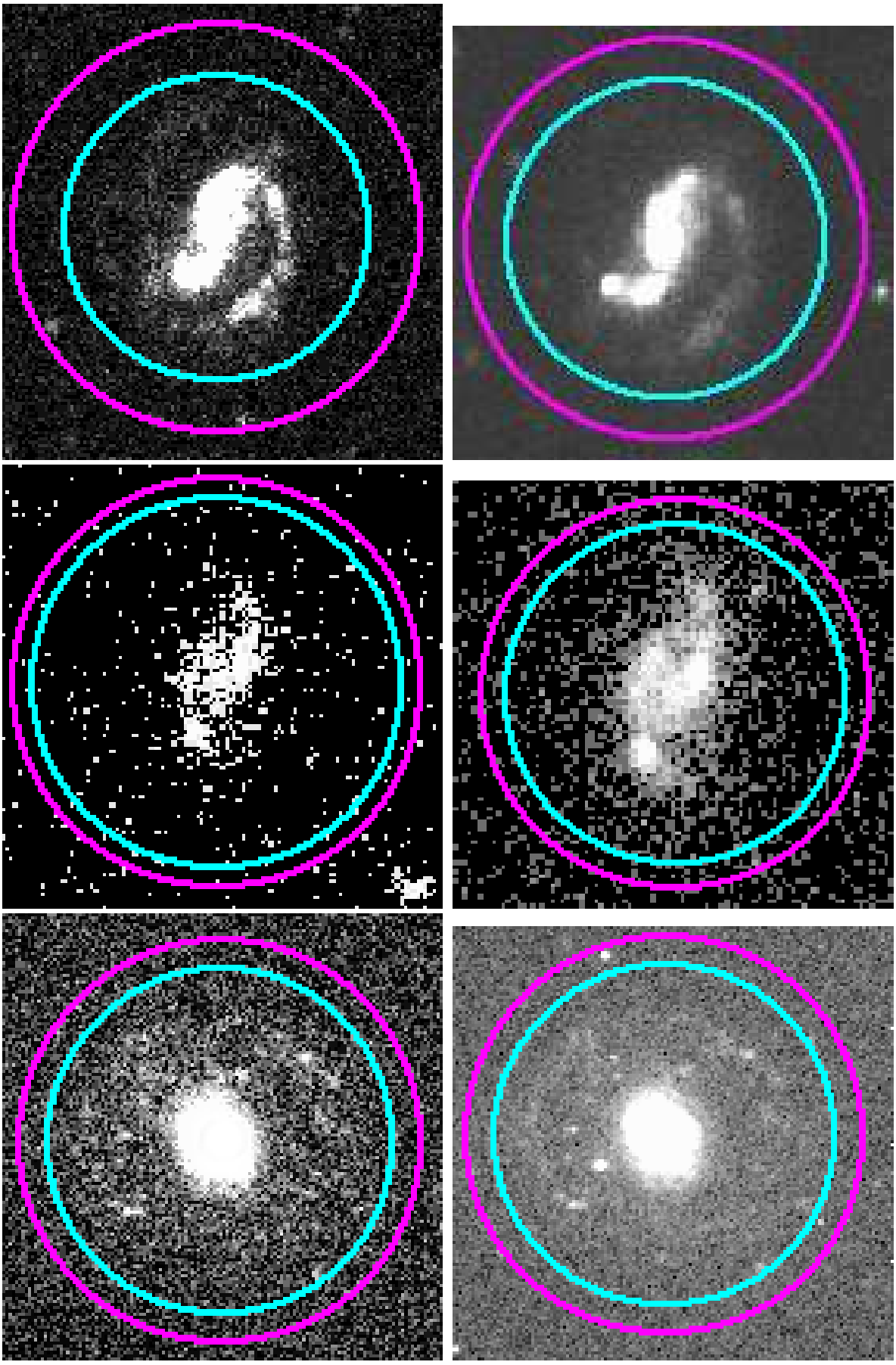

Figure 2.6: Fits images from left to right and top to bottom of NGC23 in FUV, NGC23 in NUV, NGC3110 in FUV, NGC3110 in NUV, NGC1068 in FUV and NGC1068 in NUV.

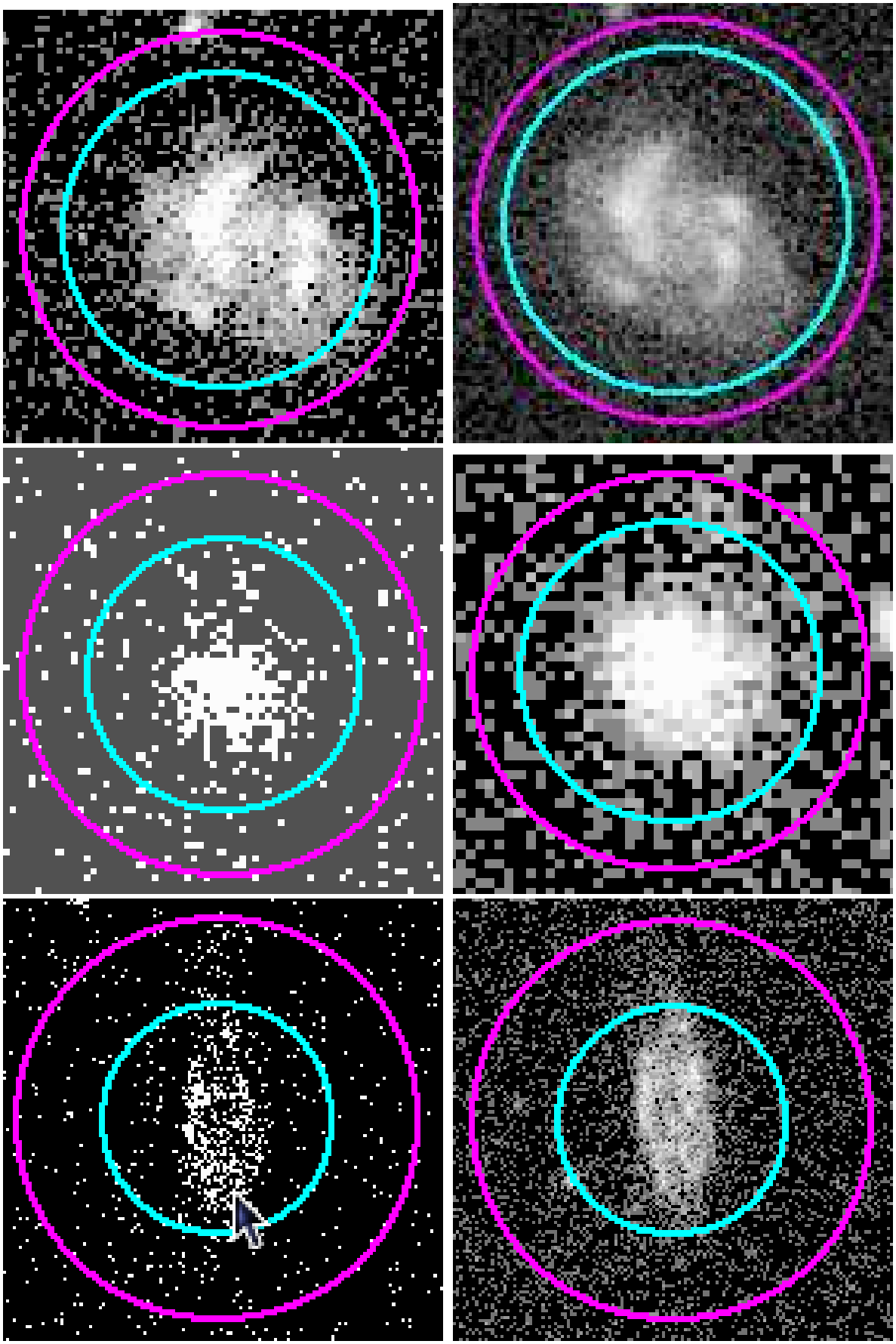

Figure 2.7: Fits images from left to right and top to bottom og NGC2342 in FUV, NGC2342 in NUV, NGC695 in FUV, NGC695 in NUV, NGC958 in FUV and NGC958 in NUV.

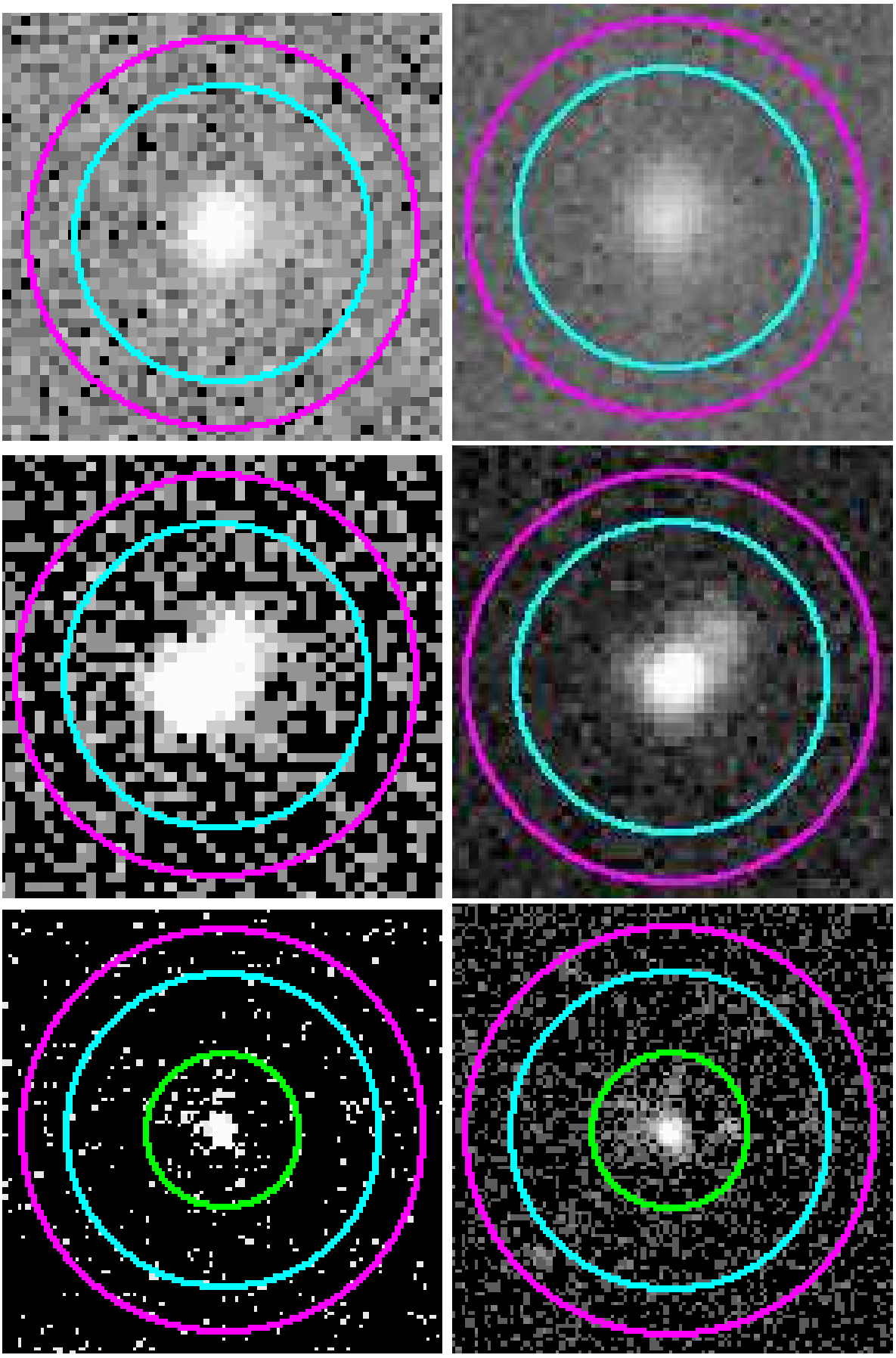

Figure 2.8: Fits images from left to right and top to bottom of IRASF23365+3604 in FUV, IRASF23365+3604 in NUV, IRASF2491-1808 in FUV, IRASF2491-1808 in NUV, IRASF15250+3608 in FUV and IRASF15250+3608 in NUV.

From figures 2.1, 2.2, 2.3, 2.4, we can see that the flux densities at the larger apertures remain constant. This is because if the calculated flux densities represent the total flux density of the galaxy since outside the galaxy, there are not any sources which belong to the galaxy and can contribute to the total flux. So, when the curve of growth flattens, it means that we reach the total flux density of the galaxy.

The calculated flux density in the FUV and NUV band, the position of the center of the object and the sizes of the apertures are presented in the tables 2.2 and 2.3.

Table 2.2: Photometry settings on FUV fits files

Galaxy	f_ν(FUV) [1]	center [2]	inner sky (″) [3]	outer sky (″) [4]
IC 1623	6058.94	(2147,2612)	40	50
NGC 877	2282.40	(3021,2556)	40	60
NGC 1365	38693.43	(3010,1830)	260	300
NGC 23	1207.97	(1920,1918)	45	60
NGC 3110	1246.74	(929,1733)	45	50
NGC 1068	27509.54	(1931,1909)	145	170
NGC 2342	2044.35	(2267,2375)	28	35
NGC 695	380.52	(1758,1043)	20	30
NGC 958	1027.95	(2843,1746)	40	70
IRAS F23365+3604	50.61	(1238,2083)	15	20
IRAS F22491-1808	177.78	(1933,1908)	15	20
IRAS F15250+3608	164.24	(1682,2525)	35	45

[1] The total flux density of the galaxy on FUV band in units of μJy
[2] The position of the galaxy's center in *atv*
[3] The inner sky of the galaxy
[4] The outer sky of the galaxy

Table 2.3: Photometry settings on NUV fits files

Galaxy	f_ν(NUV) [1]	center [2] (x,y)	inner sky (″) [3]	outer sky (″) [4]
IC 1623	7811.37	(2147,2612)	40	50
NGC 877	3451.18	(3022,2553)	40	70
NGC 1365	52492.38	(3010,1830)	260	300
NGC 23	2294.45	(1919,1919)	40	50
NGC 3110	2569.78	(929,1733)	35	40
NGC 1068	49728.14	(1931,1909)	145	170
NGC 2342	3680.26	(2271,2367)	30	35
NGC 695	705.05	(1758,1040)	15	20
NGC 958	1941.09	(2844,1742)	40	70
IRAS F23365+3604	103.57	(1238,2083)	15	20
IRAS F22491-1808	248.88	(1930,1907)	15	20
IRAS F15250+3608	321.66	(1681,2526)	35	45

[1] The total flux density of the galaxy on NUV band in units of μJy
[2] The position of the galaxy's center in *atv*
[3] The inner sky of the galaxy
[4] The outer sky of the galaxy

To test the accuracy of our measurements, we compare the flux densities with the published data of Howell et al. (2010). They measure the UV fluxes inside apertures of typical radius of 1′. Little difference was found between the fluxes of the 5 LIRGs and 3 ULIRGs. But, for the rest of the galaxies which are the most extended sources, the difference is greater because we used larger apertures than the ones of Howell et al. (2010), so we have a more correct measurement of the total UV flux density of these galaxies.

2.3 Aperture Correction

In this section we presented the procedure of the photometry aperture correction. The photometry aperture correction is a method to calculate the total flux of a point-like object.

A point-like source is an object which cannot be resolved by the instrument and the telescope. This object can be the unresolved cores of the galaxies, or galaxies which exist in extreme distances. We know that ULIRGs are compact galaxies but we do not know if they are unresolved in the *GALEX* images. For that reason, we apply aperture correction photometry to these galaxies.

In particular, we use the method of the aperture correction to obtain the total flux density of an unresolved object measuring only the flux density inside an aperture smaller than the size of the object. Then we correct the flux density with a factor, which corresponds to the aperture, and obtain the total flux density. These coefficients, which depend on the size of the aperture, arise from the aperture photometry of a known point-like source which is a star. We obtain the images of a star from the *GALEX* database. Measuring the total flux density of the star and dividing with the flux density inside an aperture we obtain the coefficient which corresponds to this aperture. This method was used on the 3 ULIRGs. Especially, the correcting factors are calculated by obtaining a star from the data of GALEX. We obtain the corrected curve of growth multiplying the flux density in each aperture with the corresponding coefficients. Finally, we put the corrected and the uncorrected curve of growth for the 3 ULIRGs in a plot which is showed in the figure 2.9.

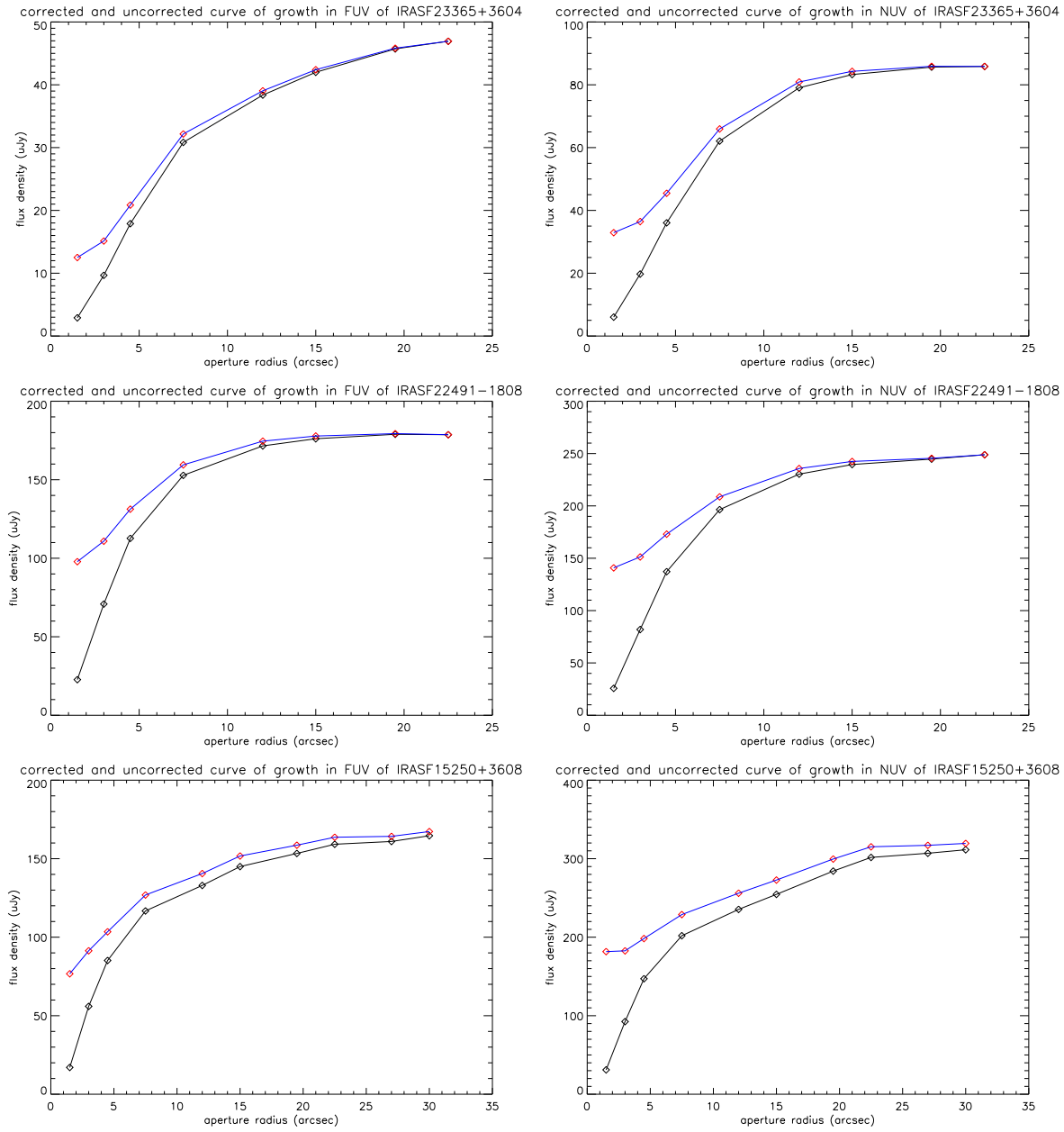

Figure 2.9: Corrected and uncorrected curve of growth from left to right and top to bottom of IRASF23365+3604 in FUV, IRASF23365+3604 in NUV, IRASF22491-1808 in FUV, IRASF22491-1808 in NUV, IRASF15250+3608 in FUV and IRASF15250+3608 in NUV.

Comparing the corrected curve of growth with the uncorrected curve of growth of the ULIRGs we see that the method of the aperture correction does not apply in apertures smaller than the size of the galaxy. We conclude that the coefficients of this method does not correct at high fraction the observed flux in order to obtain the total flux of the galaxy. So, the ULIRGs are not unresolved objects.

Chapter 3

Results

In this chapter, I combined the measurements of the UV photometry with the IR photometry values of Armus et al. (2009) in order to study the physical properties of (U)LIRGs.

3.1 Infrared Excess and β(GALEX) slope

As was discussed in the introduction, the power source of (U)LIRGs is a circumnuclear starburst and/or an AGN. These regions radiate UV light which a fraction of its absorbed by the surrounding dust and re-rariated in the FIR spectrum. So, if we want to investigate the properties and the evolution of these galaxies we have to study the UV and the IR light.

Studies which investigate UV and IR light for normal starburst galaxies were made in 1999 by Meurer et al. (1999). Sub-LIRG starburst galaxies show a strong correlation between their FIR-to-FUV flux ratios (defined as the IR excess, IRX) and their ultraviolet spectral β slopes. This relation is referred as the 'starburst' relation by Meurer et al. (1999).

This correlation comes from the following:

In normal galaxies, a fraction of the UV light which comes from young stars reaches the Earth's surface. Young stars are located in the spiral arms of the galaxy. The rest of the UV light is absorbed by the dust which is located in the spiral arms, too. In the center of normal galaxies there is a small amount of young stars and the contribution of UV light is negligible. So, it is obvious that the UV and IR light have a correlation in normal galaxies. The relationship between the β parameter and the ratio of FIR and UV fluxes is used to account for the dust in galaxies.

In order to calculate the IRX, we use the FIR fluxes from the L_{IR}, the total IR luminosity from 8 to 1000 μm and the luminosity distances. These measurements are taken from Armus et al. (2009).

Generally, the β parameter is the UV spectral slope determined from a power-law fit to the UV continuum of the form:

$$f_\lambda \propto \lambda_\beta$$

where f_λ is the flux density per wavelength interval and λ is the central rest wavelength by Meurer et al. (1999). In our case, the UV continuum slope β , respectively on (GALEX) data, is defined by Kong et al. (2004) as :

$$\beta(\text{GALEX}) = \frac{log(f_{FUV}) - log(f_{NUV})}{log(\lambda_{FUV}) - log(\lambda_{NUV})}$$

where f_{FUV} and f_{NUV} are the flux densities per unit wavelength on FUV and NUV bands respectively and λ_{eff} is the effective wavelength on each band.

It is worth testing where the 12 galaxies of the sample lie. Specifically, if there is a correlation between IR and UV luminosities of the local (U)LIRGs with $z \lesssim 0.1$, we can use the correlation for (U)LIRGs which exist at higher redshifts. As we discussed in the previous chapters, at $z \sim 1$ and $z \sim 2$, LIRGs and ULIRGs respectively are the dominant populations contributing to the star formation activity. According to the scenario that some starburst galaxies transition from LIRGs to ULIRGs to QSO hosts, if we can understand the IRX-β(GALEX) plot, we can obtain information about the evolution of these galaxies.
We calculate the β(GALEX) and the IRX for the 12 galaxies and show the results in figure 3.1.

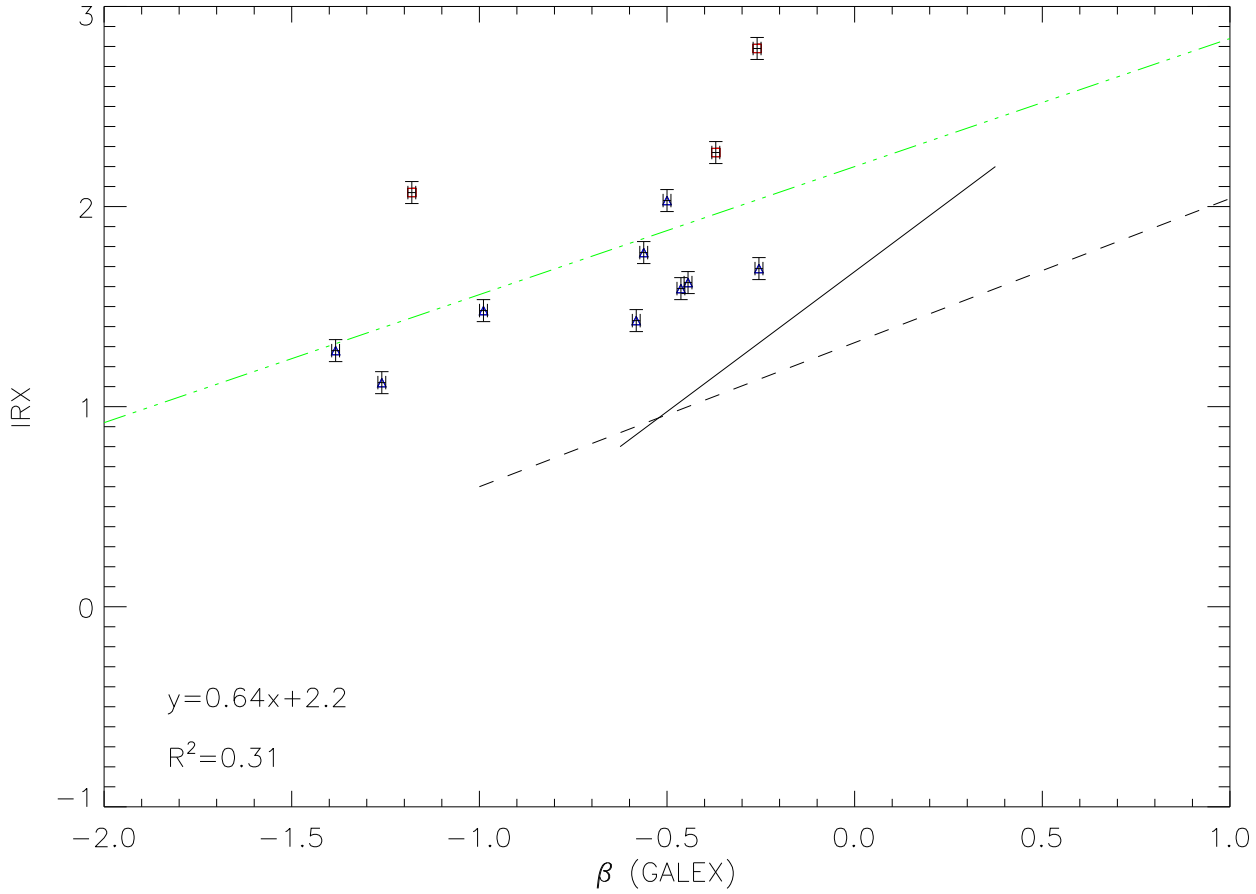

Figure 3.1: Plot of the β(GALEX) slope against the IRX. The blue triangles represent the LIRGs while the red cubes represent the ULIRGs. The solid line presents the starburst relation of Meurer et al. (1999), the dotted line is the fit to the late-type galaxy sample of Cortese et al. (2006) and the green line is the linear regression of the 12 (U)LIRGs. The equation of the linear regression and the correlation coefficient (R^2) are presented in the bottom left of the plot.

From figure 3.1 we can conclude that if we try to measure the F_{IR} from the UV light using the starburst relation, it will be underestimated. Howell et al. (2010) find the same result. The expression of the linear regression of the (U)LIRGs we measure is $y = 0.64x + 2.2$. Also, the coefficient of determination, or correlation coefficient, (R^2) is equal to 0.31 . We conclude that IRX and β(GALEX) of these galaxies do not have a strong correlation.

Moreover, the 12 galaxies of the sample lie above the starburst relation of Goldader et al. (2002). The explanation for this is that in addition to the normal starburst galaxies, in active galaxies [like (U)LIRGs] a big fraction of the energy comes from a small central region. There the dust, which is in huge amounts, absorbs a large fraction of UV light and the contribution to the observed UV decreases. So, there is no correlation of IRX-β in these galaxies. There is a decoupling between UV and IR in (U)LIRGs. We can parameterize the decoupling between UV and IR as the deviation above the starburst relation. This deviation is defined as ΔIRX. Specifically, ΔIRX indicates the extent to which the IR and UV fluxes are decoupled. We measure ΔIRX for the 12 galaxies and use the ΔIRX measurements from 10 normal galaxies [with $\leq 10^{11} L_{\odot}$; Gil de Paz et al. (2007)]. In figure 3.2 we present the plot of the $\log(L_{IR}/L\odot)$ against ΔIRX.

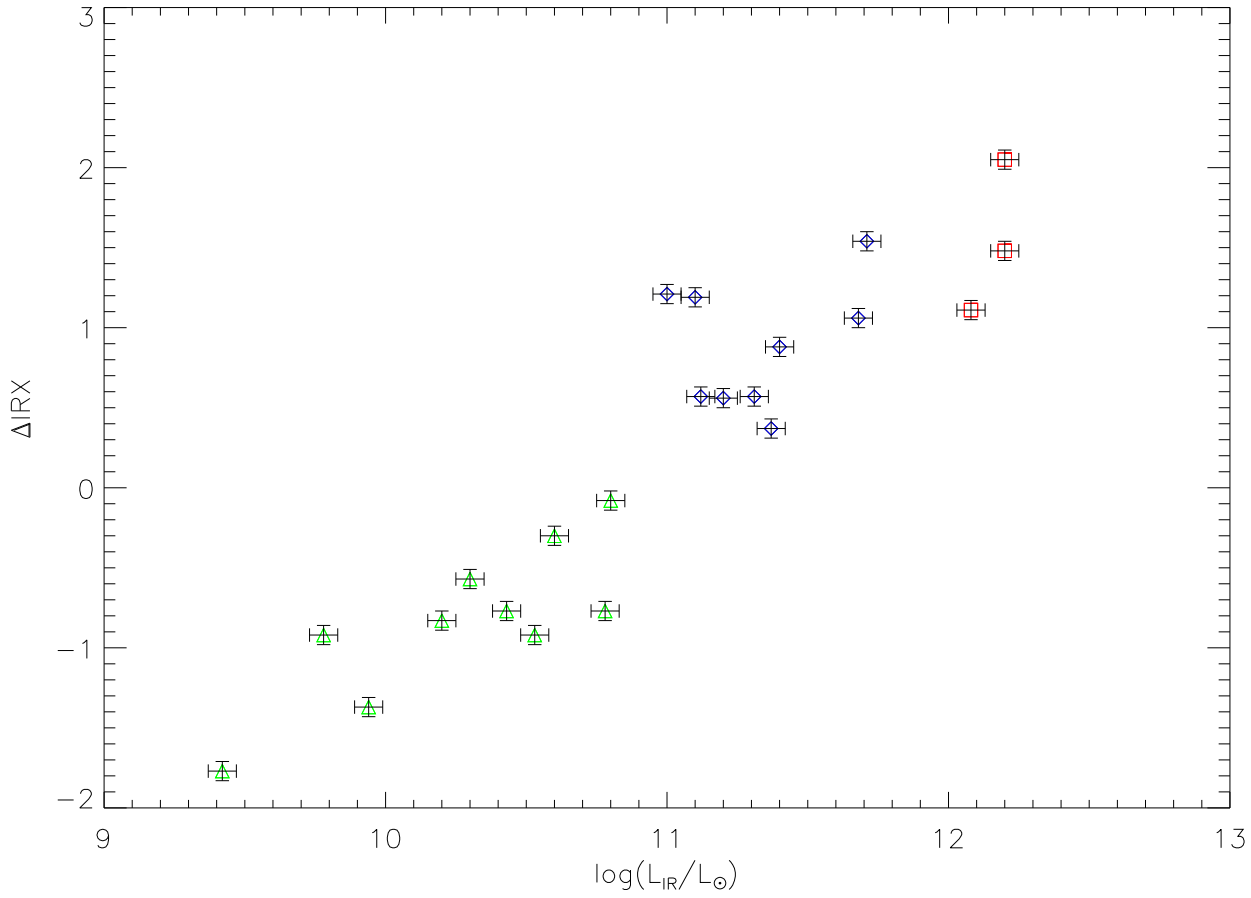

Figure 3.2: Plot of log(L_{IR}/L$\odot$) against ΔIRX. The green triangles represent the 10 normal galaxies from Gil de Paz et al. (2007), the blue squares represent the LIRGs and the red squares represent the ULIRGs.

Figure 3.2 shows that when the IR luminosity increases, from normal starburst galaxies to LIRGs and ULIRGs, ΔIRX increases with some scatter. According to Charlot & Fall (2000) the trend that (U)LIRGs have greater IRX than the normal starburst galaxies as well as the fact that ΔIRX increases from LIRGs to ULIRGs, is explained as a sequence of the optical depth. This means that the extinction for LIRGs and ULIRGs increases with the IR luminosity. So, the dust content of galaxies increases with the luminosity.

Since the dependence of ΔIRX on IR luminosity has been established, our next step will be to examine the correlation of ΔIRX with the UV emission of the 12 (U)LIRGs. For this reason, we present the ΔIRX as a function of $\log(L_{FUV}/L_{\odot})$ and $\log(L_{NUV}/L_{\odot})$ in figures 3.3 and 3.4 respectively.

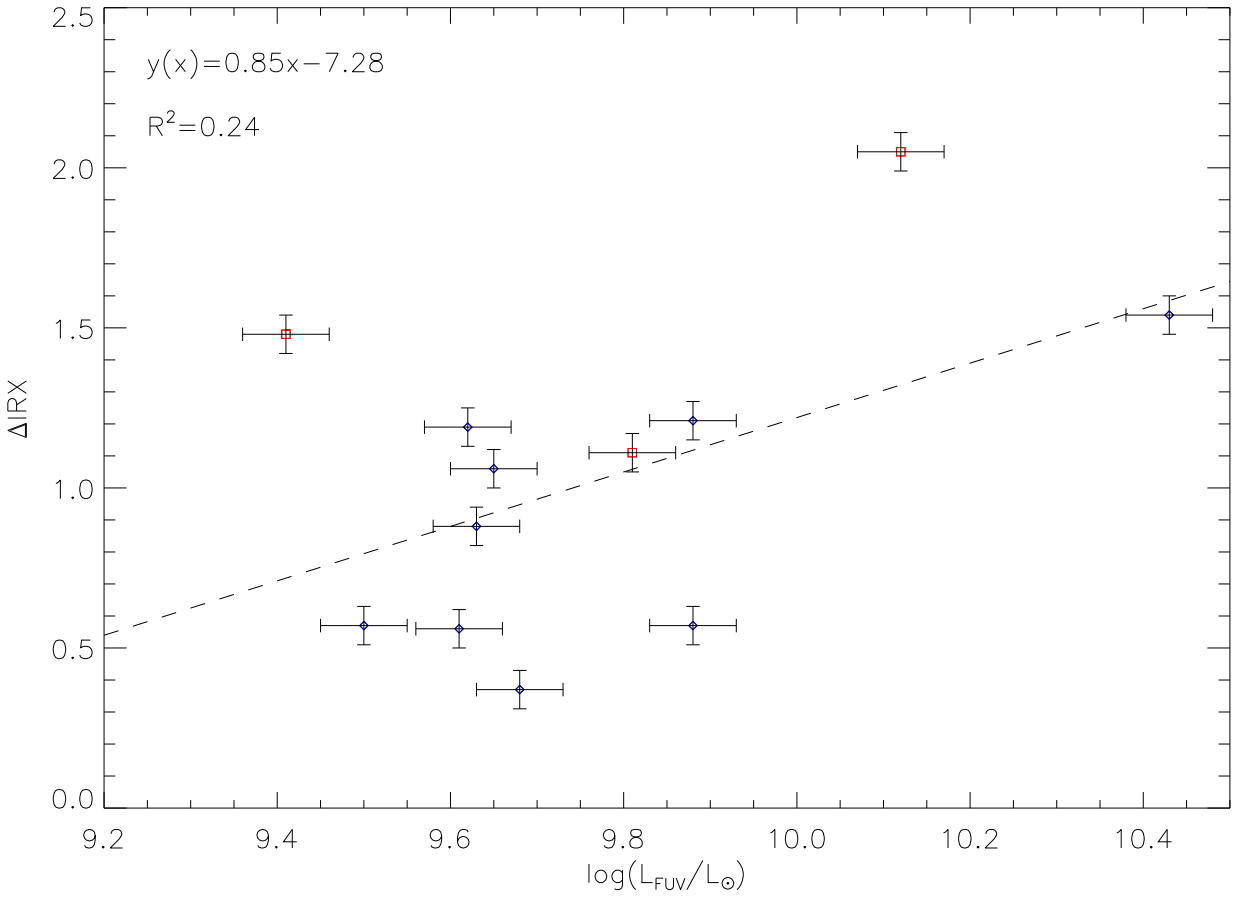

Figure 3.3: Plot of $\log(L_{FUV}/L_{\odot})$ against ΔIRX. The blue points represent the LIRGs and the red squares represent the ULIRGs. The dashed line is the linear regression of the 12 (U)LIRGs. The equation of the linear regression and the correlation coefficient (R^2) are presented on the top left of the plot.

In fig 3.4 we can see the $\log(L_{NUV}/L_{\odot})$ as a function of ΔIRX.

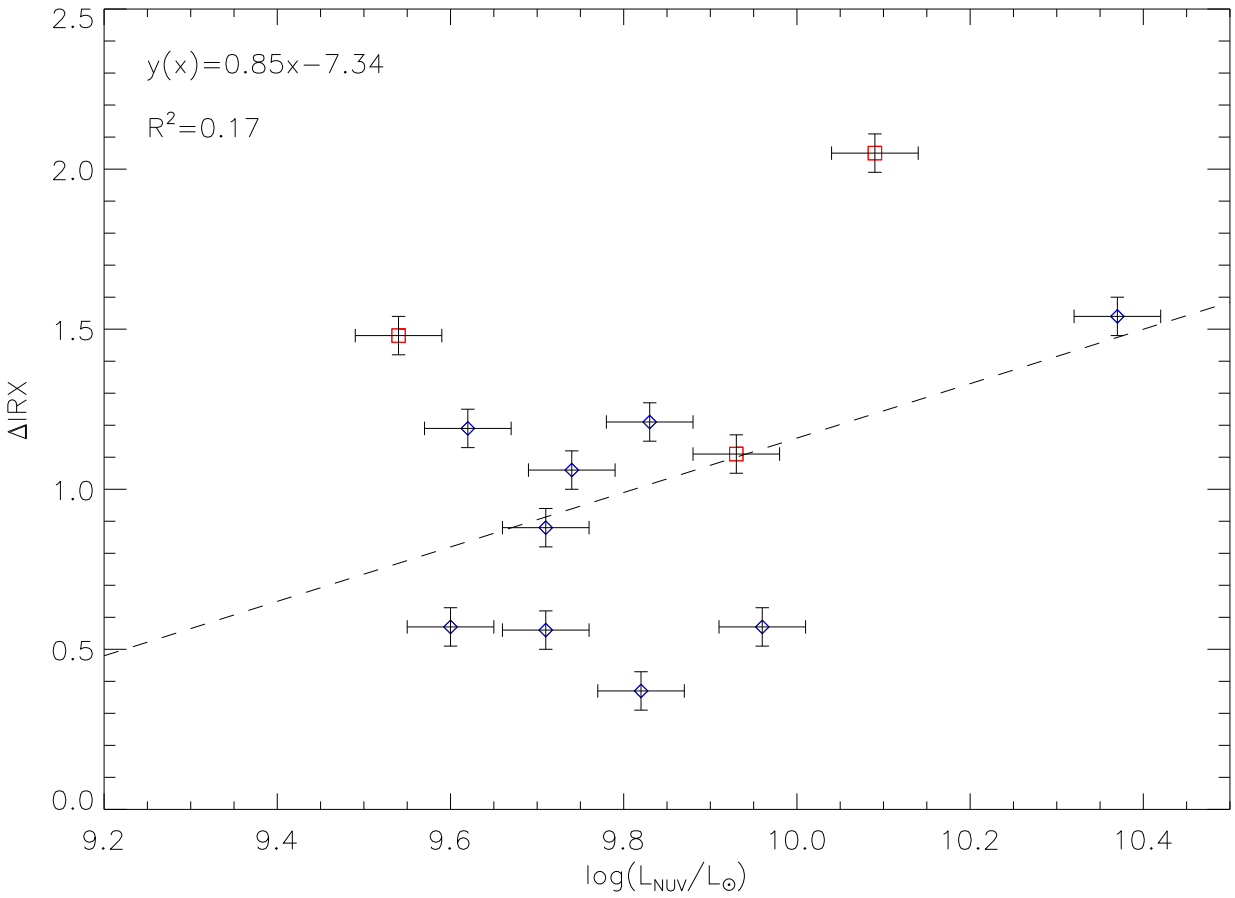

Figure 3.4: Plot of $\log(L_{NUV}/L_{\odot})$ against ΔIRX. The blue points represent the LIRGs and the red squares represent the ULIRGs. The dashed line is the linear regression of the 12 (U)LIRGs. The equation of the linear regression and the correlation coefficient (R^2) are presented on the top left of the plot.

Checking the expressions of the linear regression and the correlation coefficients for the (U)LIRGs in figures 3.3 and 3.4 (which are $y = 0.85x - 7.28$; R^2=0.24 and $y = 0.85x - 7.34$; R^2=0.17 respectively) we conclude that in addition to the correlation of ΔIRX with L_{IR}, ΔIRX in FUV and NUV bands does not seem to be related. This fact comes in agreement with the calculations of Howell et al. (2010). Also, Howell et al. (2010) did not find any correlation between ΔIRX and the following quantities: (IRAS 25μm/60μm , IRAS 60μm/100μm , Spitzer 8μm/24μm) and UV luminosity in 1600 Å ($L_{1600\mathring{A}}$) for the GOALS galaxies. Based on these calculations we can conclude that this lack of correlations between ΔIRX and global parameters other than L_{IR} suggests that the decoupling between IR and UV light takes place on small regions in most (U)LIRGs. These regions are well below the resolution of GALEX and Spitzer which is almost 6 arcsecs. If we convert this resolution in distance, it can be seen that these regions are on sub-kpc scales. Hopefully, the next missions of Herschel and HST telescopes which have better angular resolutions will investigate in more detail these small regions.

3.2 Star Formation Rates

As mentioned before, the SFR of (U)LIRGs is very high in comparison to normal galaxies. There are many ways to obtain the SFR of a galaxy using a region or a combination of regions of its spectrum. In the case of (U)LIRGs, to estimate the ongoing SFR we need to measure the direct and re-radiated stellar emission of young stars which correspond to the UV and IR light. Dust absorbs the UV light that is emitted by young stars and re-emmits it in the IR part of the spectrum and so, both wavelengths are major indicators of SFR.
We calculate the SFR in units of $M_\odot$ yr^{-1} from the IR light using the formula from Kennicutt (1998):

$$\mathrm{SFR}=4.5 \cdot 10^{-44}\, \mathrm{L}_{FIR}$$

where L_{FIR} is in units of $\mathrm{erg\,s^{-1}}$. This equation is a result of the model of Leitherer & Heckman (1995) for continuous starbursts of age 10-100 Myr with IMF interpreted as a power law:

$$\phi(m)=\frac{dN}{dm}=\mathrm{C}\cdot \mathrm{m}^{-a}$$

between the upper and lower cutoff masses (M_{up} and M_{low}) with values of $100M_\odot$ and $1M_\odot$ respectively. The normalization constant (C) is determined by the total mass converted into stars and the coefficient (a) that has value of 2.35. The IMF of Kennicutt (1998) represents a Salpeter one.
In addition, for the estimation of the SFR in units of $M_\odot$ yr^{-1} from the UV light we used the relation of Salim et al. (2007).

$$\mathrm{SFR}=1.08\cdot 10^{-28} \cdot \mathrm{L}_{FUV}$$

where L_{FUV} is the rest frame monochromatic FUV luminosity at 1528Å without absorption
in units of $\mathrm{erg\,s^{-1}\,Hz^{-1}}$.
Salim et al. (2007) suggested this equation using UV data from GALEX for local galaxies (z∼0.1) He used the Chabrier (2003) IMF with metallicity of 0.8 $Z_\odot$.
However, the SFR has been calculated using the observed (with the absorption) luminosity in order show how much each one of the following methods corrects the SFR.

The two following methods were used:
The first method comes from the paper of Buat (2005).
In particular, he measured the dust attenuation in the FUV band (A_{FUV}) using the dust to UV flux ratio. The flux of dust remission, F_{dust}, is obtained from the IR luminosity of 8-1000μm. This ratio is a quantitative measure of the dust attenuation at UV wavelengths. The formulae used here are obtained for the GALEX bandpasses:

$$A_{FUV} = -0{,}0333\ y^3 + 0{,}3522\ y^2 + 1{,}1960\ y + 0{,}4967$$

where $y = \log(F_{dust}/F_{FUV})$. The units are in erg s^{-1} cm^{-2}.
Furthermore, we calculate the apparent magnitude without the absorption (m_{real}) using the equation:

$$m_{real} = m_{observed} - A_{FUV},$$

and convert it in flux density in the AB magnitude system :

$$m(AB) = -2.5log(f) - 48.60$$

Finally we calculate the flux on FUV multiplying the flux density with the frequency of the FUV band.
The 2nd method comes from the paper of Wijesinghe et al. (2010).
They use the β(GALEX) slope to correct the FUV luminosities. The UV luminosities are dust-corrected for starburst galaxies using the following relation

$$A_{1600} = 4.43 + 1.99\ \beta$$

from Meurer et al. (1999), where A_{1600} is the attenuation at 1600Å.
Accordingly, the relation for the FUV luminosity correction is:

$$L_i = 10^{0.4(4.43+1.99\beta)}\ L_o$$

where L_i and L_o are the FUV dust corrected and uncorrected luminosities.
In the next table, we present the calculations of the SFR obtained by Kennicutt (1998) and Salim et al. (2007) with uncorrected and corrected FUV luminosities.

Table 3.1: Results of SFRs

Galaxy	SFR_{IR} [1] $M_\odot$ year^{-1}	$SFR_{UV uncorrected}$ [2] $M_\odot$ year^{-1}	$SFR_{UV corrected}$ [3] $M_\odot$ year^{-1}	$SFR_{UV corrected}$ [4] $M_\odot$ year^{-1}
IC 1623	88.30	5.73	27.02	58.69
NGC 877	21.67	0.87	8.39	13.06
NGC 1365	17.22	1.60	9.39	12.49
NGC 23	22.70	0.66	17.46	12.89
NGC 3110	40.36	1.02	37.24	22.38
NGC 1068	43.25	0.90	19.04	23.25
NGC 2342	35.15	1.61	32.88	21.68
NGC 695	82.41	0.95	22.42	41.05
NGC 958	27.29	0.87	22.02	15.73
IRAS F23365+3604	272.87	0.54	19.71	118.64
IRAS F22491-1808	272.87	2.82	19.12	134.28
IRAS F15250+3608	206.99	1.37	41.03	97.49

Table 3.2: [1] Star formation rates derived from Kennicutt relation using IR luminosities from Armus et al. (2009). [2] Star formation rates derived from Salim et al. (2007), using uncorrected FUV luminosities. [3] Dust corrected star formation rates derived from Salim et al. (2007) using FUV luminosities. The dust correction UV emission is derived using the β(GALEX) from Wijesinghe et al. (2010). [4] Dust corrected star formation rates derived from Salim et al. (2007) using FUV luminosities. The dust correction UV emission is derived using the formula for dust extinction from Buat (2005).

The SFR of the (U)LIRGs is extremely high compared with the ones of normal starburst galaxies which have values of 1-3 $M_\odot$ yr^{-1}. The SFR calculated from IR luminosity is on average 94.25 $M_\odot$ yr^{-1}. In addition, the uncorrected SFR from FUV light is very low compared with the SFR from IR light. Especially, the $SFR_{UV uncorrected}$ has a mean value of 1.58 $M_\odot$ yr^{-1}. So, the FUV emission without dust-correction contributes on a small fraction of SFR, on average 1.7%. This is because the UV emission is absorbed by dust.

If we try to correct the FUV light for dust attenuation we see that generally the SFR_{UV} increases considerably but never reaches the values of SFR based on the IR light. Calculating the mean values of the dust corrected, SFR from FUV emission from β(GALEX) and from Buat (2005) increases (on average) up to 24.37% and 50.54% respectively of the SFR_{IR} for the 12 (U)LIRGs. In particular, the SFR from FUV emission, using the dust correction of Buat (2005), is higher than the SFR which is corrected from β(GALEX) slope for the 8 of the 12 galaxies.

The mean values of the SFR in LIRGs are 24.58 $M_\odot$ yr^{-1} and 21.76 $M_\odot$ yr^{-1} from Buat (2005) and β(GALEX) respectively. So, the contributions of the 2 methods on LIRGs give almost the same results.

But, when we correct the FUV light for ULIRGs, the mean value of SFR from Buat (2005) is 116.80 $M_\odot$ $year^{-1}$ while the mean value of SFR from β(GALEX) slope is only 26.62 $M_\odot$ $year^{-1}$. From this we conclude that the β slope is a rough indicator of the dust attenuation of UV light for the ULIRGs, leading to less accurate and flawed dust corrections than the dust correction method of Buat (2005).

Ideally, if we knew the fundamental equations for the calculation of the SFR from UV and IR light, the ratio of $\frac{SFR(_{IR})}{SFR(_{UV})}$ would be equal to unit. In the next figure 3.5 the ratio of $\frac{SFR_{IR}}{SFR_{UV corrected}}$ against $\log(L_{IR}/L_\odot)$ is represented, where the SFR_{IR} is calculated from the Kennicutt (1998) formula and the $SFR_{UV corrected}$ is calculated from Salim et al. (2007) with dust correction from the method of Buat (2005).

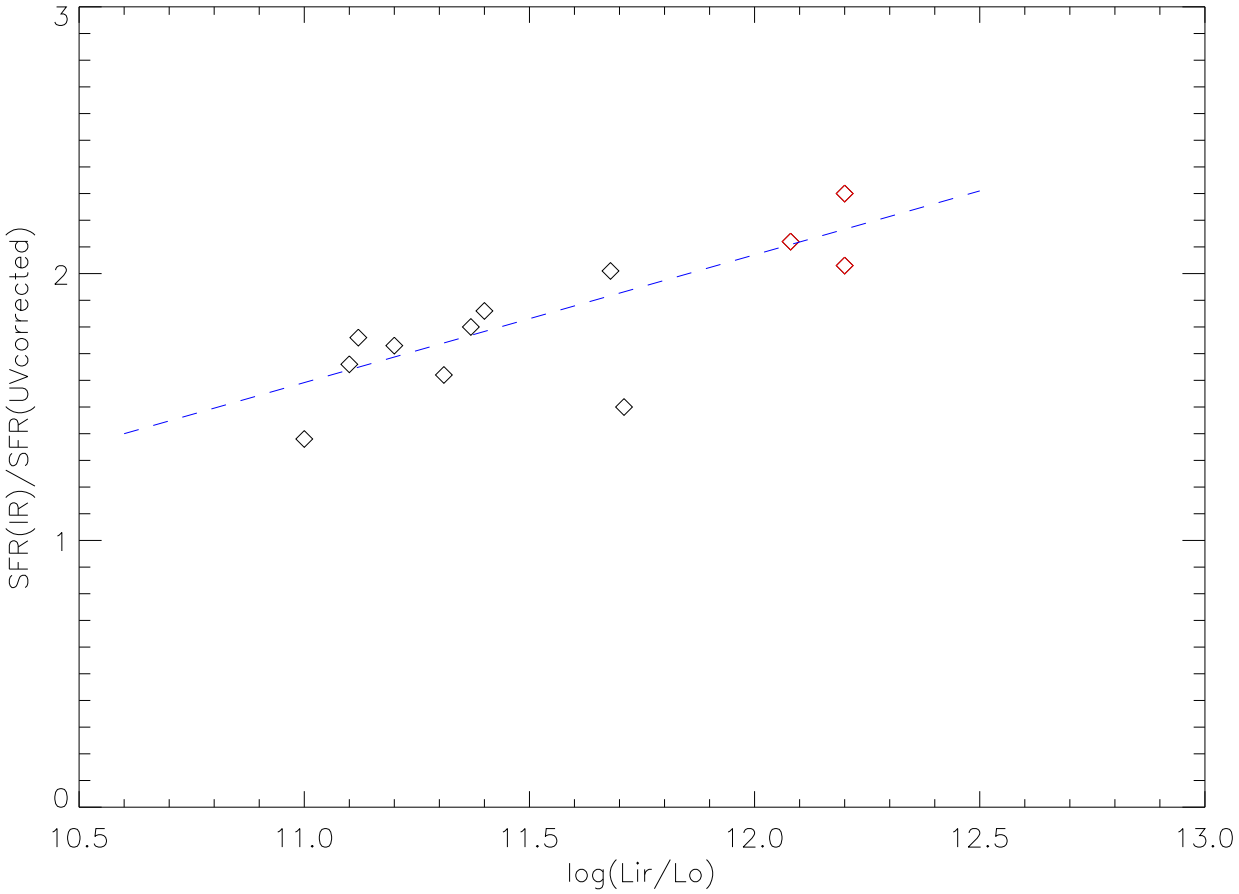

Figure 3.5: Plot of the ratio $SFR_{IR}/SFR_{UVcorrected}$ against $\log(L_{IR}/L_{\odot})$. The SFR_{IR} is calculated from the Kennicutt (1998) formula and the $SFR_{UVcorrected}$ is calculated from Salim et al. (2007) with dust correction from the method of Buat (2005). The black squares represent the LIRGs while the red squares represent the ULIRGs. The dashed line is the linear regression of the 12 (U)LIRGs.

The equation of the linear regression and the correlation coefficient (R^2) of the plot in figure 3.5 are $y = 0.48x - 3.69$ and R^2=0.62. We see that there is an increase in the ratio of $\frac{SFR_{IR}}{SFR_{UV corrected}}$ as the L_{IR} increases. This means that the UV luminosity, as the galaxy is more luminous in IR, does not contribute to its energy even if it is corrected by the absorption. The galaxy becomes optically thick in UV light. The dust inside the galaxy absorbs a high fraction the UV luminosity from the young stars while the IR luminosity becomes higher.

Chapter 4

Conclusions

In this thesis, we measure the UV fluxes of 12 (U)LIRGs of the GOALS sample. Combining the UV measurements with the IR flux values from Armus et al. (2009) we find the following results:

1. (U)LIRGs have large IRX compared to the normal starburst galaxies. On average, more luminous (U)LIRGs have larger IRX. Thus, more luminous (U)LIRGs are more extincted than less luminous (U)LIRGs.

2. Using the starburst relation of Meurer et al. (1999) to estimate L_{IR} from the UV measurements of (U)LIRGs would underestimate L_{IR}.

3. The ΔIRX of (U)LIRGs increases with L_{IR}. This means that the decoupling between IR and UV emission becomes greater from LIRGs to ULIRGs. The contribution of the UV luminosity to the observed UV emission decreases when the galaxy becomes more IR luminous.

4. Calculating the SFR using the UV emission, we conclude that for (U)LIRGs, FUV emission without dust-correction contributes to a small fraction of SFR, on average 1.7%. After correcting the FUV emission from β(GALEX) and from Buat (2005), the SFR increases, on average, up to 24.37% and 50.54% respectively of the SFR_{IR}. Also, the Buat (2005) correction method is more reliable for (U)LIRGs than the one with β(GALEX). Thus, β(GALEX) is not a good dust indicator for the sample, especially for ULIRGs.

5. The ratio of $\frac{SFR_{IR}}{SFR_{BuatUVcorrected}}$ increases while the L_{IR} increases for (U)LIRGs.The SFR_{UV} becomes less important as the L_{IR} increases.

Bibliography

Armus, L., et al. 2009, *PASP*, 121, 559

Aussel, H., Vigroux, L., Franceschini, A., Elbaz, D., Dennefeld, M., & Cesarsky, C. J. 1999, in Bulletin of the American Astronomical Society, Vol. 31, Bulletin of the American Astronomical Society, 1386–+

Barnes, J. E. 1992, *ApJ*, 393, 484

Buat, V. 2005, in American Institute of Physics Conference Series, Vol. 761, The Spectral Energy Distributions of Gas-Rich Galaxies: Confronting Models with Data, ed. C. C. Popescu & R. J. Tuffs, 297–306

Caputi, K. I., et al. 2007, *ApJ*, 660, 97

Chabrier, G. 2003, *PASP*, 115, 763

Charlot, S., & Fall, S. M. 2000, *ApJ*, 539, 718

Chary, R., & Elbaz, D. 2001, *ApJ*, 556, 562

Cortese, L., et al. 2006, *ApJ*, 637, 242

Dopita, M. A., & Sutherland, R. S. 1995, *ApJ*, 455, 468

Draine, B. T. 2003, *ARA&A*, 41, 241

Elbaz, D., Cesarsky, C. J., Chanial, P., Aussel, H., Franceschini, A., Fadda, D., & Chary, R. R. 2002, *A&A*, 384, 848

Elbaz, D., et al. 1999, *A&A*, 351, L37

Franceschini, A., Aussel, H., Cesarsky, C. J., Elbaz, D., & Fadda, D. 2001, *A&A*, 378, 1

Genzel, R., et al. 1998, *ApJ*, 498, 579

Gil de Paz, A., et al. 2007, *ApJS*, 173, 185

Gisler, G. R. 1980, *AJ*, 85, 623

Goldader, J. D., Meurer, G., Heckman, T. M., Seibert, M., Sanders, D. B., Calzetti, D., & Steidel, C. C. 2002, *ApJ*, 568, 651

Ho, L. C., Filippenko, A. V., Sargent, W. L. W., & Peng, C. Y. 1997, *ApJS*, 112, 391

Howell, J. H., et al. 2010, *ApJ*, 715, 572

Kennicutt, Jr., R. C. 1998, *ARA&A*, 36, 189

Kong, X., Charlot, S., Brinchmann, J., & Fall, S. M. 2004, *MNRAS*, 349, 769

Lagache, G., et al. 2004, *ApJS*, 154, 112

Le Floc'h, E., et al. 2005, *ApJ*, 632, 169

Leitherer, C., & Heckman, T. M. 1995, *ApJS*, 96, 9

Mazzarella, J. M., Graham, J. R., Sanders, D. B., & Djorgovski, S. 1993, *ApJ*, 409, 170

Metcalfe, L., et al. 2003, VizieR Online Data Catalog, 340, 70791

Meurer, G. R., Heckman, T. M., & Calzetti, D. 1999, *ApJ*, 521, 64

Mirabel, I. F., Lutz, D., & Maza, J. 1991, *A&A*, 243, 367

Reuland, M. 2005, PhD thesis, Leiden Observatory, Leiden University, P.O. Box 9513, 2300 RA Leiden, The Netherlands

Rieke, G. H., et al. 2004, *ApJS*, 154, 25

Salim, S., et al. 2007, *ApJS*, 173, 267

Sanders, D. B., Mazzarella, J. M., Kim, D.-C., Surace, J. A., & Soifer, B. T. 2003, *AJ*, 126, 1607

Sanders, D. B., & Mirabel, I. F. 1996, *ARA&A*, 34, 749

Sanders, D. B., Soifer, B. T., Elias, J. H., Madore, B. F., Matthews, K., Neugebauer, G., & Scoville, N. Z. 1988b, *ApJ*, 325, 74

Sanders, D. B., Soifer, B. T., Elias, J. H., Neugebauer, G., & Matthews, K. 1988a, *ApJ Lett.*, 328, L35

Tacconi, L. J., Genzel, R., Lutz, D., Rigopoulou, D., Baker, A. J., Iserlohe, C., & Tecza, M. 2002, *ApJ*, 580, 73

Wijesinghe, D. B., et al. 2010, ArXiv e-prints

Wilson, A. S., Braatz, J. A., Heckman, T. M., Krolik, J. H., & Miley, G. K. 1993, *ApJ Lett.*, 419, L61+

L.S.Sparke & J.S.Gallagher,III, *Galaxies in the Universe* (Cambridge University Press)

B.W.Caroll & D.A.Ostlie *An Introduction to Modern Astrophysics* (Addison-Wesley)

S. Clark, *Towards the Edge of the Universe* (Wiley 1997)